Adsorption phenomena and surface interactions between superplasticisers and ground blast furnace slag and metakaolin particles in alkali solutions: implications for low-carbon cements

M.R.C. da Silva[a]*, J. Qi[a], I. M. Ross[a], A. P. Kirchheim[b], B. Walkley[a]*

[a] School of Chemical, Materials, and Biological Engineering, University of Sheffield, UK

[b] Department of Civil Engineering, Federal University of Rio Grande do Sul, BR

* Corresponding authors: micaelrubens@gmail.com. b.walkley@sheffield.ac.uk.

Abstract

The performance of superplasticisers in alkali-activated materials (AAMs) remains poorly understood, limiting the wider adoption of low-carbon cement technologies. This study examines the behaviour of lignosulfonate- (LS), naphthalene- (NP), and polycarboxylate ether (PCE)-based superplasticisers in $NaOH/Na_2SiO_3$-activated systems with ground granulated blast furnace slag (GGBFS) and metakaolin (MK). The adsorption phenomena and polymer conformation were investigated by combining mini-slump tests (flow behaviour), ATR-FTIR (chemical interactions), DLS (polymer size), TEM-EDX (polymer conformation), zeta potential measurements (surface charge), and total organic carbon analysis (polymer uptake). Results show that in both GGBFS and MK systems, high alkalinity alters polymer ionisation, suppresses electrostatic interactions, reduces superplasticiser solubility, and drives polymer agglomeration. In GGBFS systems, Ca^{2+} enhances superplasticiser adsorption to solid particles. LS-based superplasticisers demonstrated superior alkaline resistance, slump retention, and adsorption capacity relative to NP and PCE. These findings provide new mechanistic insights to guide the design of high-performance superplasticisers tailored for low-carbon AAM systems.

Keywords: Superplasticisers**.** Chemical admixtures. Surface interactions. Adsorption phenomena. Ground granulated blast furnace slag. Metakaolin. Alkali-activated materials.

1. Introduction

Chemical admixtures are substances added in small quantities to concrete formulations to enhance specific characteristics in both the fresh and hardened states. Amongst them, superplasticisers are used as dispersant polymers that adsorb onto the surface of cement particles. Their primary function is to enhance workability and flow characteristics of cementitious materials by promoting particle dispersion through electrostatic repulsion or steric hindrance without adding extra water to the concrete mix [1]. As modern concrete increasingly incorporates chemical admixtures, controlling their effective performance is essential, particularly in the development of sustainable 'low-carbon' cementitious materials with reduced clinker factor, high incorporation of supplementary cementitious materials (SCM), and more complex pore solution chemistry. The mechanisms governing the reduced performance of conventional superplasticisers in low-carbon cements are not fully understood. Consequently, the chemical industry faces challenges in producing commercial superplasticisers for cements with low clinker factor and high SCM content that are as effective as those designed for conventional/ordinary Portland cement (OPC).

Alkali-activated materials (AAMs) are a form of low-carbon cement that with lower associated CO_2 emissions than conventional PC. These materials are produced through a chemical reaction between solid aluminosilicate precursors and alkaline solutions (activators) that undergo an alkali-activation process [2]. When superplasticisers are added to AAM mixes, they are exposed to an aqueous phase with high alkalinity (pH) and ionic strength, which differs considerably from the aqueous chemistry of fresh hydrated OPC. Consequently, the surface interactions between solid cement particles and superplasticisers will differ from those in OPC systems and are influenced by factors such as the type of precursors, activators, and superplasticisers.

AAMs can be classified into two groups based on the precursor's calcium (Ca) content: High-Ca AAMs or Low-Ca AAMs (also called geopolymers) [3]. In the high-calcium AAMs, e.g., with ground granulated blast furnace slag (GGBFS), the main mechanisms of superplasticiser interaction with GGBFS particles are dictated by Ca^{2+} ions. Using a synthetic pore solution of OPC with GGBFS, Habbaba and Plank [4] identified the presence of an electric double layer (EDL) on the slag surface. This EDL comprised a positively charged Stern layer due to the adsorption of ions Ca^{2+} from cement and slag, with a negatively charged diffuse layer filled

with SO_4^{2-} ions. Since an EDL has been attributed to high Ca AAMs, the superplasticiser would gradually adsorb onto the surface of the slag via these Ca-bridge sites.

In the case of low-calcium (or calcium-free) systems, such as with metakaolin (MK), the superplasticiser-particle interaction mechanisms will differ due to a lack of divalent cations (e.g., Ca^{2+}) to facilitate polymer adsorption by shifting the surface charge of MK particles from negative to positive. According to Derkani et al. [5], in a study using a naphthalene-based superplasticiser, there is a competition between these superplasticisers and water for sites on the MK surfaces. Less-hydrated cations disturb the interfacial water structure around MK particles during these interactions. Therefore, superplasticiser polymers can interact with MK's amorphous gel-like surface layer and surface groups. Additionally, the blocking of reactive sites, the characteristics of the EDL, and the water molecules created will promote repulsion between the MK particles.

The type of activators also affects the interactions of superplasticisers in AAMs. Sodium hydroxide (NaOH) and sodium silicate (Na_2SiO_3) are examples of common activators for alkaline activation. They provide the alkali media of the solutions (high pH), which alter the initial surface charges of GGBFS or MK particles, as determined by zeta potential measurements. From pH 7 to 12, MK particles have highly negative zeta potential values, whereas GGBFS can exhibit either positive or negative zeta potential values depending on their chemical composition [6,7]. Beyond pH 12, these materials dissolve in the high pH environment and release different ions (Si, Al, Ca, Mg, etc.), leading to zeta potential values towards the isoelectric point. Simultaneously, this dissolution also leads to a greater ionic concentration, which can affect the solubility of the superplasticiser [8]. Sodium silicate-based activators (Na_2SiO_3), can negatively affect the fluidity of AAM mixes due to their high viscosity [9]. The impact of Si ions on zeta potential values needs further investigation.

As pH increases, the activators dissociate into Na^+, OH^-, and SiO_3^{2-} ions, altering the ionic strength and chemistry of the aqueous phase, and consequently the surface interactions between superplasticiser molecules and solid precursor particles. OH^- ions are likely to interact with other superplasticiser groups or surfaces by electrostatic interactions. Na^+ and Ca^{2+} ions can facilitate the adsorption of polymers onto solid precursor particle surfaces due to their positive nature. Vanitha et al. [10] studied alkali-activated fly ash (FA)/GGBFS-based systems with sodium silicate, nanosilica, and modified polycarboxylate, confirming that Na and Ca ions

change the zeta potential charges to less negative values. However, this phenomenon is more pronounced with divalent cations such as Ca^{2+} when compared to Na^{+} [5].

The most common commercial superplasticisers are based on lignosulfonate (LS), sodium naphthalene sulfonate formaldehyde (NP), Melamine (M), and polycarboxylate ether/ester (PCE) polymers. They contain a mix of different polymers and secondary products, such as defoaming agents, to mitigate the negative effect of air in the concrete mix. LS consists of randomly branched polyelectrolyte macromolecules in a lignin structure – phenyl propane units connected with C-C bonds [11]. The resulting cross-linked structure has a molecular weight ranging between 100g/mol to 400,000 g/mol [12]. The LS-based superplasticisers are mainly composed of sulfonate groups, but many other functional groups can be found, such as carboxylic acid, sulfonic acid phenolic hydroxyl, methoxyl, or a combination of these [13]. NP is a dispersant commercialised in liquid or powder form as sodium or calcium salts [1]. They are synthesised in processes involving sulfonation of naphthalene from the reaction of β-naphthalene sulfonates with formaldehyde in acid solutions to form the anionic polymers [1,14]. They have a lower molecular weight (around 1000 to 20,000 g/mol), reaching a higher dispersion after 5 repeating molecules [1,15]. M-based superplasticisers are not studied in this study.

Polycarboxylate-ether (PCE) polymers are synthetic macromolecules characterised by a backbone composed of carboxylate groups, with pendant side chains extending from the main chain, which give them a “comb-like” structure. The versatility of PCE-based superplasticisers arises from the ability to modify various molecular features, including the backbone chemistry, molecular weight, side chain length, degree of anionicity, and specific structural motifs. These modifications influence the polymer conformation in solution (manifesting as train, loop, or tail structures), the adsorption layer thickness, and the performance of the superplasticisers in different media [16]. These structural differences amongst different superplasticisers influence their chemical stability, conformation, and interaction with precursor particles in highly alkaline systems.

The current state-of-the-art describes the superplasticiser-particle interactions depending on the type of superplasticiser and the particle’s surface characteristics. Kalina et al. [17] described the interactions of LS-based superplasticisers in alkali-activated slag concrete (AAS), which is driven by electrostatic repulsion. The negative sulfonate groups in LS polymers adsorb on the positive surface of slag due to the deprotonation of silanol groups. Electrostatic repulsion is

also the proposed working mechanism in NP-based superplasticisers [18–20]. In the case of the PCE-based superplasticisers, steric hindrance caused by the side chain is known as the main mechanism for particle dispersion. Wang et al. [21] present a schematic representation to describe the structure of superplasticiser LS-, NP- (referred to as PNS in the article), and PCE-based superplasticisers and their interactions of fly ash (FA) particles in AAMs, as shown in Fig. 1. Their findings revealed various weak interactions, involving the hydrogen bonding with electron cloud of aromatic rings and silanol -OH groups (illustrated with green dashed lines), which would be predominant in LS- or NP-based superplasticisers, as well as between hydroxyl groups and oxygen atoms within functional groups such as sulfonate, carboxyl, phenolic, and polyoxyethylene chains (pink dashed lines), existing in all superplasticisers. The Ca^{2+} facilitating the binding of superplasticisers is an established interaction mechanism cited by several authors in AAS studies with LS-, NP-, and PCE-based superplasticisers [10,21,22]. These Ca^{2+} function as connectors between the negatively charged functional groups of superplasticisers and oxygen-containing sites. However, spatial constraints hinder some portions of the superplasticiser molecules (monomers and oligomers) from effectively reaching all reactive regions on the FA surface. Moreover, the simultaneous interaction of superplasticisers and developing gel phases for these active locations may delay the reaction kinetics.

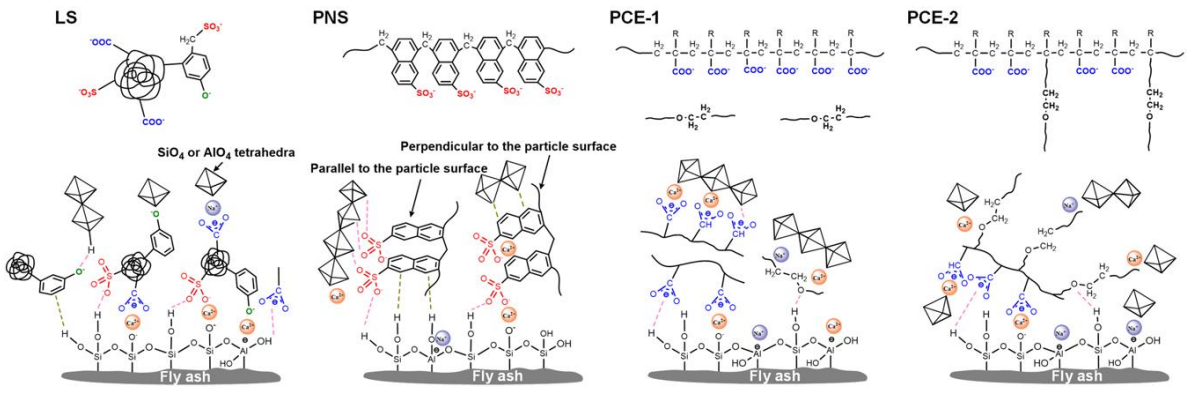

Fig. 1. Interactions between Lignosulfonate (LS)-, polynaphthalene(PNS)-, Polycarboxylate1 (PCE1), and polycarboxylate2(PCE2)-based superplasticisers and species in FA-based alkali-activated pastes [21].

Despite advancements in the last decades of understanding these surface interactions, the complex chemical environments of AAMs continue to challenge the design of effective admixtures. Chemically simplified solutions AAM-relevant (presence of SiO_3^{2-}, Na^+, or OH^-) can help provide some insights into the factors impacting the effectiveness of superplasticisers.

Also, it is worth studying whether Ca^{2+} ions could be a strategy to enhance the adsorption ability of different superplasticisers in alkali-activated systems, as it has been described in previous studies [23,24]. In the literature, gaps still remain in regard to how to systematically predict the superplasticiser performance, the conformation of different superplasticisers in the aqueous phase of fresh AAMs, how the interactions amongst different superplasticisers and particles affect the zeta potential, and other interactions with MK or GGBFS particles in varied aqueous solutions with LS, NP or PCE-based superplasticisers. The majority of the progress in this field has been focused on the PCE-based superplasticisers for AAS systems, and the interactions between superplasticisers and MK particles in AAMs have been overlooked. There are also few studies investigating the reduced effectiveness of varied superplasticisers (LS, NP, or PCE) with SCM particles in simplified pore solutions and at the nanoscale. Chen and Plank [25] attributed the reduced effectiveness of PCEs in AAS to a limited polymer adsorption onto the GGBFS surfaces in NaOH solution and almost no adsorption in Na_2SiO_3 pastes. According to the authors, the media jeopardises the adsorption of PCE polymers, which therefore coil and agglomerate. Although no image evidence of the agglomeration polymers has been presented yet. This highlights the need for a deeper understanding of superplasticiser behaviour in these systems, which will support the broader adoption of AAMs in sustainable construction.

The research presented here addresses these gaps by examining the behaviour of LS-, NP-, and PCE-based superplasticisers in highly alkaline environments using NaOH + Na_2SiO_3 relevant alkali-activated systems. It uses chemically simplified solutions to gain insights into the reduced effectiveness of superplasticisers in AAMs, and explores superplasticiser chemical stability, agglomeration, and adsorption phenomena in the presence of common solid precursors (GGBFS and MK) and varied alkalinity with electrolytes relevant to different AAMs chemistries (SiO_2, NaCl, $CaCl_2$). The findings contribute new knowledge to aid the development of next-generation superplasticisers tailored for high-performance low-carbon cements. Through a combination of spectroscopic, microscopic, and electrokinetic analyses, the research seeks to clarify how alkaline conditions and precursor type affect polymer performance, with the broader objective of identifying strategies to enhance superplasticiser efficacy and compatibility in low-carbon AAM systems.

178 # 2. Materials and methods

179 ## 2.1. Materials characterisation

180 Commercial GGBFS (EcoCEM) and MK (Metamax, BASF) were used as solid aluminosilicate
181 precursors to produce particle dispersions and alkali-activated cement samples. The particle
182 size distribution (PSD) of each solid precursor was measured by laser granulometry (using a
183 Malvern Mastersizer) in triplicate with 60 seconds of ultrasound per repetition and dispersion
184 of the particles in isopropanol (GGBFS) or water (MK). The specific surface area was
185 measured via the adsorption of nitrogen gas using the BET method (SSA_{BET}), with a heating
186 rate of 20 °C/min in a nitrogen gas atmosphere. The chemical composition was measured by
187 X-ray fluorescence (XRF) in a Sequential X-ray fluorescence spectrometer between 400 and
188 4000 cm^{-1} wavelengths. All characterisation data for the precursors are presented in Table 1.

189 Table 1: Characterisation of the precursors

Characterisation	Ground Granulated Blast Furnace Slag (GGBFS)	Metakaolin (MK)
D_{v90} (µm)	22.60	13.80
D_{v50} (µm)	10.00	4.49
D_{v10} (µm)	2.14	1.45
Span ($\frac{D_{v90}-D_{v10}}{D_{v50}}$)	2.03	2.60
SSA_{BET} (m^2/g)	1.43	12.48
Oxide compositions (wt.%) as determined by X-ray fluorescence analysis		
SiO_2	36.00	52.54
Al_2O_3	11.30	44.54
Fe_2O_3	0.30	0.36
CaO	41.80	<0.05
MgO	6.50	-
SO_3	0.70	-
TiO_2	0.50	1.31
K_2O	0.4	0.15
Na_2O	0.1	0.21
Others*	-	0.2

LOI	1.9	0.63
Total (%)	100	100

*including MnO, Cr, etc.

The alkaline activator solutions used sodium hydroxide in pellets (NaOH, putirty 99%) and a sodium silicate solution (H_2O= 55.9%, Na_2O= 14.7, and SiO_2= 29.4%). The simplified alkaline solutions used to mimic AAM-relevant solutions used sodium hydroxide (NaOH, purity 99%), silica oxide (SiO_2, 99%), sodium chloride (NaCl, >95%), and calcium chloride ($CaCl_2$, 97%). Six commercial superplasticisers were used in this study: two lignosulfonate-based (LS) (**LS1** and **LS2**), one poly(naphthalene sulfonate)-based (**NP1**), one mixture of lignosulfonate+naphthalene polymers (**LS+NP**), and two poly(carboxylate-ether)-based superplasticisers (PCE) (**PCE1** and **PCE2**). The technical information of these superplasticisers is presented in Table 2.

Table 2: Technical information of the superplasticisers according to the suppliers

ID	Base	pH	Density [kg/l, 20°C]	Colour	Recommended dosage [wt. % of binder]	Solid content (%)
LS1	Modified lignosulfonate	5.0 ± 1.0	1.18	Brown liquid	0.3-0.7 %	~ 40
LS2	Modified lignosulfonate	-	1.19	Dark brown liquid	0.3-0.8 %	~ 40
NP1	Naphthalene condensate	-	1.26	Dark brown liquid	0.8- 3.0 %	~ 37
LS+NP	Modified lignosulfonates and naphthalene condensate	5.0 ± 1.0	1.17	Brown liquid	0.3-1.0 %	~ 30
PCE1	Modified polycarboxylate	3.6± 1.0	1.05	Pale brown liquid	0.2-1.5 %	~ 29
PCE2	Modified polycarboxylate	3.6± 1.0	1.08	Amber liquid	0.3-1.0%	~32

Fig. 2. (a) shows the PSD of the superplasticisers in deionised (DI) water as determined via Dynamic Light Scattering (DLS) using a NANO-flex® II system with 180° DLS. The measurements were performed in suspensions of 10 µL of superplasticisers dispersed in 100 mL of DI water. The results show a steric size of 20-400 nm, 4-20 nm, 100-800 nm, and 0-10 nm for LS, NP, LS+NP, and PCEs, respectively.

Attenuated total reflectance Fourier Transform infrared spectroscopy (ATR-FTIR) was used to collect the data regarding bonding environments in the superplasticisers. Analysis involved placing a few drops of each superplasticiser on the FTIR-ATR diamond crystal. The samples were analysed in a range of 400 to 4000 cm-^{1}, using a Thermo Fisher Nicolet iS5 FTIR spectrometer equipped with a Specac Golden Gate Single Reflection Diamond ATR System, KBr optics, a diamond ATR crystal, and ZnS lenses. Each spectrum will be an average of 64 scans with a spectral resolution of 2 cm^{-1}. Fig. 2 (b) shows the resulting FTIR data for each superplasticiser. LS-based superplasticisers exhibit peaks at 1510 cm^{-1} (aliphatic cyclic hydrocarbons, –C–C) and 1032 cm^{-1} (sulfonic acids, S–O), while NP shows characteristic sulfonate (S–O) peaks at 1180, 1120, and 1033 cm^{-1}, and PCE presents additional peaks at a band around 1460–1080 cm^{-1} range, assignable to ether (C–O–C) vibrations [26,27].

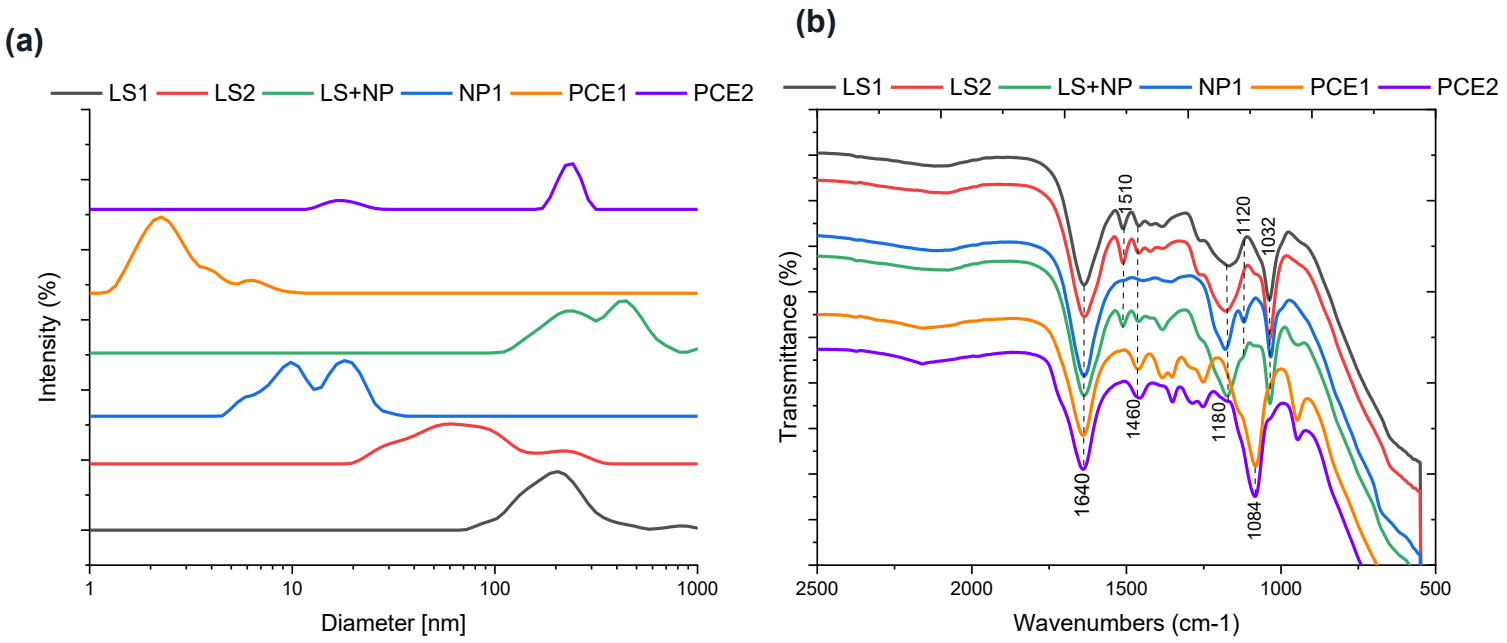

Fig. 2. (a) Particle size distribution data obtained via DLS measurements and (b) ATR-FTIR data for each superplasticiser as marked.

2.2 Experimental design

The experimental programme of this study is structured into two main parts. The first part (i) involves investigating the dispersion performance of commonly used commercial superplasticisers (LS, NP, or PCE types) in AAMs formulated either with GGBFS or MK as precursors and a combination of NaOH and Na_2SiO_3 as activators. In this phase, mini-slump tests were conducted to assess the dispersing effectiveness of each superplasticiser. These tests also served as a preliminary screening step to identify three of each type of superplasticiser that produced the highest paste spread in the GGBFS- or MK-based AAM systems, which were then selected for more in-depth analysis in the second part of the programme.

The second part (ii) focuses on elucidating the underlying mechanisms by which superplasticisers interact with AAM systems and on identifying the key factors that influence their reduced performance at the tested dosage. This was achieved using chemically simplified solutions designed to represent the characteristic chemical environments of low-calcium (MK-based) and high-calcium (GGBFS-based) AAM systems activated with NaOH and Na_2SiO_3. The simplified approach enabled a more fundamental investigation of the interactions between superplasticiser molecules and solid surfaces under controlled chemical conditions, allowing for the identification of the role of each constituent.

The overall experimental design is illustrated in Fig. 3. The left side of the figure outlines the main variables controlled throughout the study, including the type of precursor material (MK or GGBFS), the superplasticiser type (LS-, NP-, or PCE-based), the type of electrolyte presents in the solution (SiO_2, NaCl, or $CaCl_2$), and the pH, which was adjusted across a range from 7 to 14 using NaOH. The right side of the figure illustrates the key possible interactions considered between superplasticiser molecules and the surface of solid particles, along with the analytical techniques employed to characterise these interactions.

Their interactions were monitored as follows: to investigate the chemical robustness of superplasticisers in alkaline media and their molecular conformation when dispersed in solution under varying alkaline conditions, a combination of ATR-FTIR, DLS, and Transmission Electron Microscopy with Energy-dispersive X-Ray spectroscopy (TEM/EDX) was used. ATR-FTIR was used to monitor chemical changes in the superplasticisers at different pH levels. DLS was employed to determine changes in steric size in solution, and TEM provided direct imaging of the superplasticiser conformation in various alkaline media. Surface charge modifications were assessed using zeta potential measurements performed across a

range of pH values and with varying concentrations of different electrolytes (0 to 0.1 M), at constant pH. These measurements enabled evaluation of the effects of pH, electrolyte type, and superplasticiser type on the surface charge behaviour of the dispersions.

Finally, the adsorption behaviour of superplasticisers onto the solid particle surfaces in the presence of Ca^{2+} (in the form of $CaCl_2$) was explored as a strategy to enhance the adsorption ability of different superplasticisers. This was investigated using a total organic carbon (TOC) test employing the depletion method. This method determined the difference between the initial TOC (before adding precursors) and the final TOC (after adding precursors) in the presence of superplasticisers, indicating the amount of organic content that has been removed due to interactions with the particle's surface. More details can be found in the section "analytical tests conducted".

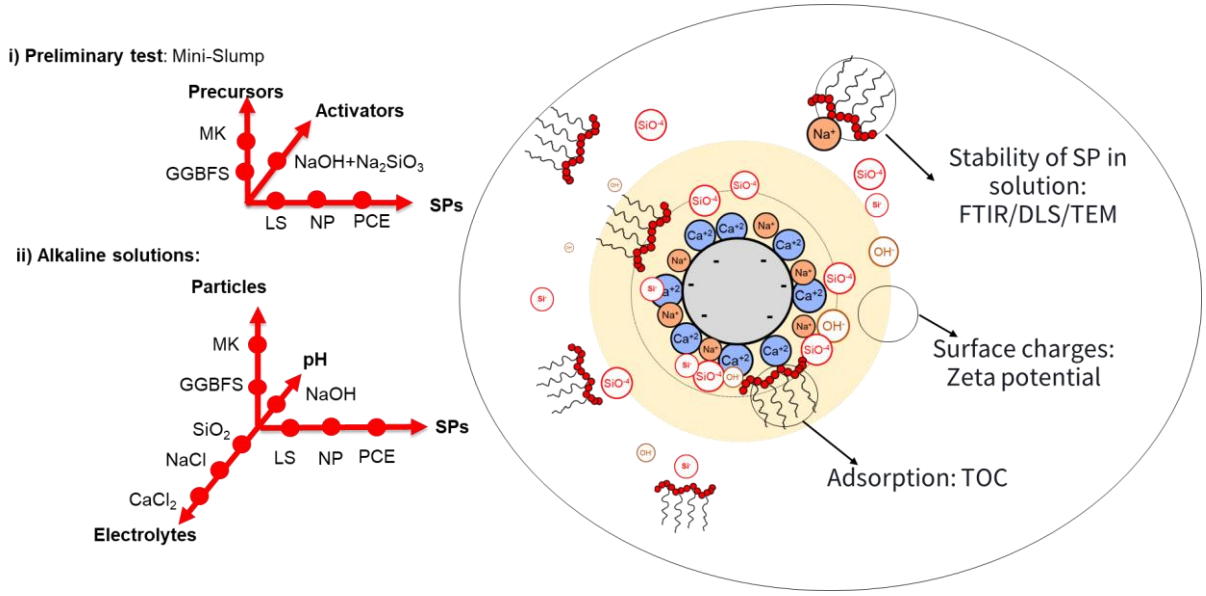

Fig. 3. Experimental programme. Top-Left: preliminary mini-slump test showing the precursors, activators, and superplasticisers used. Bottom-left: Sample matrix showing the parameters investigated in the alkaline solutions, including particle type, solution pH, superplasticiser type, and electrolyte type and concentration. Right: techniques used to investigate the particle surface interactions in chemically simplified solutions.

2.3 Sample preparation

2.3.1 AAM

AAMs were prepared from either MK or GGBFS powders, and a sodium silicate solution, prepared using NaOH and Na_2SiO_3 reagents, based on formulations from previous studies

[28,29]. AAMK was formulated with SiO_2/Na_2O=1.5, Al_2O_3/Na_2O=1.0 and H_2O/Na_2O=13 molar ratios. AAS was prepared by mixing 4g og NaOH pellets and 3.86g of Na_2SiO_3 commercial solution with 100g of GGBFS, and a water-to-solids ratio (w/s) of 0.42. The alkaline solutions were prepared by dissolving NaOH pellets into deionised (DI) water and a Na_2SiO_3 solution. The solutions were left to equilibrate at room temperature for 24 hours before the mixing procedure. The precursors, alkali solution, and 1% superplasticiser (wt.% precursor) were added to a beaker and simultaneously mixed with an overhead mixer (Heidolph, RZR2020) at 2000 rpm for 10 min to achieve homogeneity, using a dissolving radial blade. The AAM formulations are presented in Table 3.

Table 3: Mix formulations of the AAMs

Mix	Precursor	Precursor mass	Na_2SiO_3 dose (g)	NaOH dose (g)	Mixing water (g)	Superplasticisers type (1.00 g)
AAMK	MK	100	107.79	14.50	38.67	LS1 LS2 NP1 LS+NP PCE1 PCE2
AAS	GGBFS	100	3.86	4.00	42	LS1 LS2 NP1 LS+NP PCE1 PCE2

2.3.2 Simplified aqueous solutions

The dilute dispersions of particles in chemically AAM-relevant simplified solutions were prepared by dispersing 1g of precursor (either MK or GGBFS) in 100 mL of alkaline solution and subsequently adding 1% superplasticiser (wt.% % of precursor). The alkaline solutions were prepared with different molar concentrations of NaOH, SiO_2, NaCl, and $CaCl_2$. Control solutions comprising suspensions of 1% of each superplasticiser in 100 mL of DI water at various pH values (7 to 14) without precursors were used. The pH values were adjusted by

adding NaOH. The effects of varied SiO_2, NaCl, and $CaCl_2$ concentrations were assessed at a fixed 1 M NaOH solution.

2.4 Analytical tests conducted

2.4.1 Mini-slump test

The effectiveness of superplasticisers on enhancing the fluidity of the AAM pastes was evaluated using a mini-slump test [30]. 6 different paste-based samples were tested: 3 superplasticisers in AAMK systems and 3 superplasticisers in AAS systems. The test was also performed as a preliminary test to select three of six superplasticisers for the aqueous solutions analysis (one of each type, i.e., one LS-, one NP-, and one PCE-based superplasticiser). The samples were mixed according to the description in Section 2.3.1. The spread diameter obtained after each test was recorded at time (t) = 0, 10, 20, 30, 40, 50, and 60 min after mixing. The spread diameter was measured with a digital calliper in two perpendicular directions (d_1 and d_2). Each result was used to calculate the relative mini-slump flow (Γp) [31] (Eq. 1), where d_0 represents the internal diameter of the cone base, and d corresponds to the average of d_1 and d_2. 1% superplasticiser (wt.% of precursor) was used. Each paste sample was tested twice, and the results are reported as the average value.

$$\Gamma p = \left(\frac{d}{d0}\right)^2 - 1, \; where \; d = \frac{d1+d2}{2} \qquad \text{Eq. 1}$$

2.4.2 Attenuated Total Reflectance-Fourier Transform Infrared (ATR-FTIR)

ATR-FTIR data were collected for the superplasticisers and the chemical stability of superplasticisers in dilute dispersions of the precursor materials and superplasticisers in chemically simplified solutions. Chemical stability is defined in this work as the capacity of the superplasticisers to resist any modifications in their chemical composition in alkaline media, which can be identified by changes in the FTIR spectra. A Thermo Fisher Nicolet iS5 FTIR spectrometer equipped with a Specac Golden Gate Single Reflection Diamond ATR System, KBr optics, and ZnS lenses was used. A few drops of each dispersion were placed on the diamond ATR crystal and then covered with a cap and subsequently analysed in a range of 400 to 4000 cm^{-1}. Each spectrum was an average of 64 scans with a spectral resolution of 2 cm^{-1}.

2.4.3 Dynamic Light Scattering (DLS)

DLS data for dilute dispersions of superplasticisers in chemically simplified solutions were obtained using a NANO-flex® II system with 180° DLS. The measurements were conducted on suspensions of 10 µL of each superplasticiser in 100 mL of DI water at various pH values (7 to 14). The pH values were adjusted by adding NaOH.

2.4.4 Transmission Electron Microscopy (TEM) with Energy Dispersive X-ray spectroscopy (EDX)

TEM was performed on the dilute dispersions of superplasticisers in chemically simplified solutions using a cold field emission gun (c-FEG) (TEM, JEOL JEM-F200), coupled with a twin solid-state, ultra-sensitive, large silicon drift detector (SDD) EDX system, operating at 200 kV. The technique was used to analyse the conformation of the superplasticiser in NaOH solution (1 M). The samples were prepared by diluting the superplasticisers (0.02-0.5 µL) in 1 mL of the relevant solution. A drop of the sample was placed on the TEM copper grid with pipettes, placed on filter paper, and stored in a desiccator for at least 24 hours to remove any free water and prevent inaccurate images and damage due to any steam.

2.4.5 Zeta potential

Zeta potential measurements of the dilute dispersions of the precursor materials and superplasticisers in chemically simplified aqueous solutions were conducted using Stabino ® II, a Colloid Metrix instrument. The technique measures zeta potential charges by inducing liquid flow via an oscillating plunger, which disrupts the ion cloud around the particles, generating a streaming potential detected by electrodes to assess dispersion stability. All data were collected at 20 °C, ambient pressure, 5 times (totalising 30 runs).

2.4.6 Total Organic Carbon (TOC)

The adsorbed amounts of the superplasticiser on the solid particles were measured using the depletion method [32]. The amount of non-adsorbed superplasticiser remaining in solution after each adsorption experiment was determined by analysing the TOC content of the solution. TOC analysis was performed using a Shimadzu Total Organic Carbon VCPH/CPN analyser. 10 mL sample solutions were filtered using syringe filters of 0.2 µm to separate solid materials remaining after 1h of stirring. The filtrate was diluted 100 times, and the data were obtained by combustion over an oxidation catalyst at 680°C using 150 mL/min zero-grade air as the

carrier gas. The results were calculated from the difference between the TOC content of the control solutions and the respective solutions according to the depletion method.

3 Results and discussion

3.1 Dispersion performance of superplasticisers in AAMs

Fig. 4 shows the mini-slump test results of AAMK and AAS pastes formulated with different superplasticisers (fixed dosage of 1wt.%), measured at 10 min, 20 min, 30 min, 40 min, 50 min, and 60 min after initial mixing. Overall, the AAMK pastes exhibited a greater spread diameter, and hence greater fluidity than AAS pastes, attributed to the higher amount of alkali liquid solution needed to induce the reaction of MK (see Table l). For AAMK pastes, the superplasticisers LS1, LS2, NP1, and LS+NP increased the spread diameter of the pastes compared to the reference samples (formulated without superplasticiser, black line) and PCE (orange and purple lines) from 10 min to 60 min.

The LS-based superplasticiser was the most effective among all superplasticisers at increasing the paste spread diameter, which aligns with previous work on superplasticisers for AAS [24]. No studies testing the workability of MK-based geopolymer with LS-based superplasticisers were found. Luukkonen et al. [24] showed LS exhibited greater paste fluidity and lower paste viscosity in AAS-based systems when compared to melamine (M), NP and PCE-based superplasticisers. According to Liu et al. and Luukkonen et al. [12,24], the abundance of sulfonate groups on these LS-based superplasticiser molecules enhances the solubility and dispersion ability as these groups attach to Na^+ or Ca^{2+} in the EDL of AAS. In the case of MK, it would be likely caused by Na^+ present in the NaOH solution.

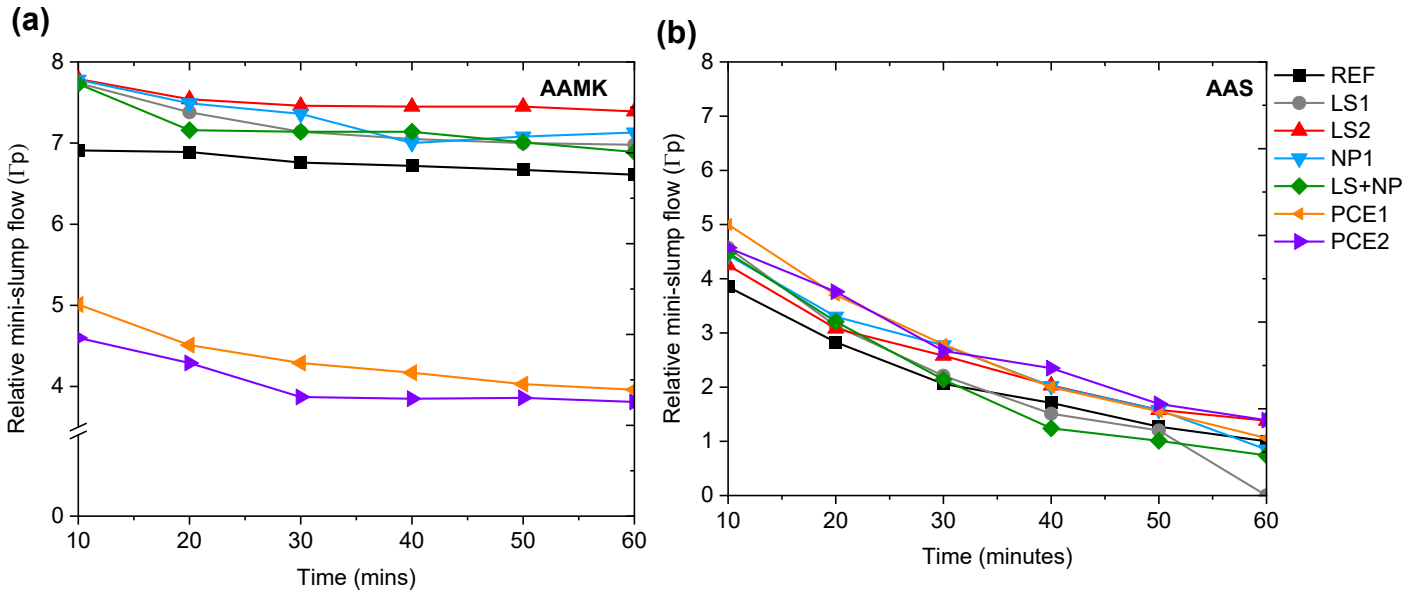

375

376 **Fig. 4.** Relative mini-slump flow (a) AAMK with different superplasticisers. (b) AAS with
377 different superplasticisers. 1% superplasticisers (wt.% of precursor). Results expressed as
378 average value.

379 Other reasons for the better dispersion ability of lignosulfonate polymers for both AAM
380 systems investigated (especially AAMK) are related to their high density, high molecular
381 weight and gel-like structure [12]. Such characteristics can make it difficult for alkaline groups
382 (e.g., hydroxide ions) to penetrate the long lignosulfonate chains, promoting the chemical
383 breakdown of the structure and changes in the solubility capacity. With more lignosulfonate
384 polymers remaining in solution, their adsorption on the MK surface will be greater (which is
385 confirmed in the TOC results of simplified solutions in the Results and Discussion section).
386 This adsorption might delay the fast dissolution of Si and Al ions from MK to form N-A-S-H
387 gel, which could also adsorb superplasticisers. The pastes with LS-based superplasticisers also
388 presented better slump retention amongst the samples, which is due to a known retarding effect
389 of LS caused by the presence of sugars and lignin structure that introduces a retarder effect in
390 cementitious materials. Although not in the scope of this study, the effect of the admixtures on
391 the reaction kinetics should be taken into consideration as one of the reasons for the different
392 spreads over time.

393 When PCE were used in the AAMK pastes, an inverted effect was observed. These samples
394 exhibited the lowest spread diameter (and hence the lowest fluidity) among the
395 superplasticisers analysed, indicating their poor performance in AAMK systems. This suggests

that PCE has lower alkali resistance compared to LS and NP in AAMK. The factors explaining the mechanisms behind this reduced dispersion ability are elucidated from the analysis of aqueous solutions in the following sections, which show the low alkaline resistance of PCE to these alkaline media.

For AAS pastes, all the superplasticisers had very similar dispersion ability. Compared to the reference (without superplasticisers), PCE-based samples exhibited a better spread diameter, indicating their performance in increasing the fluidity of the AAS pastes over time. At 10 min, PCE1 and PCE2 increased the spread diameter by an average of 30% and 19%, respectively, relative to the reference sample. At this time LS1, LS2, NP1, and LS+NP had similar performance, increasing the spread diameter in average 15%. After 60 minutes, PCE2, LS2, and PCE1 exhibited a spread diameter greater than the reference sample by an average of 6%, 39% and 38%. Meanwhile, LS1 and LS+NP had a performance inferior to the reference sample. The improved efficiency of PCE-based superplasticisers in AAS compared to AAMK systems may result from the greater calcium content of the AAS reaction mixture of AAM produced from calcium-rich precursors (such as GGGBFS).

To explain this behaviour, previous work has experimentally determined the thermodynamic parameters affecting the adsorption performance of PCE molecules in the presence of calcium ions [32]. Plank, Sachsenhauser, and de Reese [32] reported that Ca^{2+} ions change the complexation state of PCEs and reduce the anionic charge of the polymers. The authors observed that in $CaCO_3$ systems, the binding of calcium ions to carboxylates or other functional groups of PCE reduces the strength of the attraction between PCE and positively charged surfaces, such as $CaCO_3$. If the charge neutralisation is sufficiently strong, electrostatic repulsion may occur, leading to a decrease or slight increase in the enthalpy contribution to adsorption. Simultaneously, the system gains entropy, which ultimately drives adsorption, even in the presence of unfavourable enthalpy changes.

Therefore, it is likely that there is an interaction between the PCE main chain adsorbed onto the GGBFS particle surfaces due to the Ca^{2+} ion bridges, and the PCE lateral side chains then promote GGBFS particle repulsion. The effects of Ca^{2+} on the adsorption ability of the different superplasticisers will be further discussed in the TOC section. From the mini-slump test, one type of each superplasticiser (LS2, NP1 and PCE1) was chosen to investigate the interactions between the solid precursor particles and the superplasticiser molecules by analysing dilute

dispersions of particles in chemically simplified solutions, resulting in three superplasticisers instead of the initial six samples.

3.2 Chemical stability and aggregation behaviour in alkaline media

3.2.1 Effects of pH via FTIR-ATR

Suspensions of superplasticisers LS2, NP1, and PCE1 with MK or GGBFS particles in alkaline solutions were prepared using NaOH ($1x10^{-6}$ M -1 M) to adjust the pH levels from 7 to 14. The ATR-FTIR results, as shown in Fig. 5, indicate that the chemical environment alters the chemical bonding interactions of superplasticisers in AAM-relevant solutions. The spectra at the top of all graphs (a-f) represent chemical admixtures without dilution in alkaline media (LS2, NP1 or PCE1), showing different bands corresponding to their chemical composition. The broader bands around 1640 cm^{-1} represent the bending vibration of hydroxyl groups[33], which is present in all samples regardless of the varied pH values, indicating the presence of water and hydroxyl interactions.

The main characteristic functional groups of superplasticisers were also identifiable. For LS-based superplasticisers (a, b), the peaks at 1511 cm^{-1} and 1032 cm^{-1} correspond to aliphatic cyclic hydrocarbons (-C-C) and sulfonic acids (S-O), respectively. NP exhibits peaks at 1180, 1120, and 1033 cm^{-1} are related to hydrophilic groups such as sulfonates (S-O) (b,e). While PCE, band around 1114 – 1180 cm^{1} can be either stretching sulfonate (S-O) or stretching of groups (C-O-C, from PCE side chains) (c,f) [26,27]. When these superplasticisers are added to an alkaline solution (from pH~11), these peaks start to reduce in intensity and disappear, which is even more pronounced as the pH increases for both suspensions. No significant differences were observed when the spectra of superplasticisers in the presence of MK/GGBFS particles were compared.

These spectral changes indicate that the molecular structure and ionisation state of superplasticisers are altered in all high-pH environments, elucidating what occurs in cement pore solutions, affecting the chemical stability of superplasticisers and their potential ability to interact with the cementitious particles. For example, the disappearance or reduction of these bands may indicate changes in conformation of superplasticisers due to rearrangement of functional groups or the backbone and side chains (case of PCEs) or even degradation of some compounds. Zhang et. al [33] investigated the effect of five superplasticisers (LS-, M-, NP-, and PCE-based superplasticisers) in fly-ash-based AAMs activated with NaOH. They observed that superplasticiser maintains performance at low NaOH concentration (0.1 M); however, as

the NaOH concentration increases, the structure of superplasticisers is destroyed into small molecules. The alterations are visible for colour alterations, agglomeration and separation of liquid and solution into distinguished layers at 5 M or 10 M NaOH concentration. This behaviour can explain the reduced effectiveness of superplasticisers in the mini-slump test, particularly for PCE in AAMK. Thus, ATR-FTIR provides critical insights into the chemical robustness of each superplasticiser type under alkaline activation conditions.

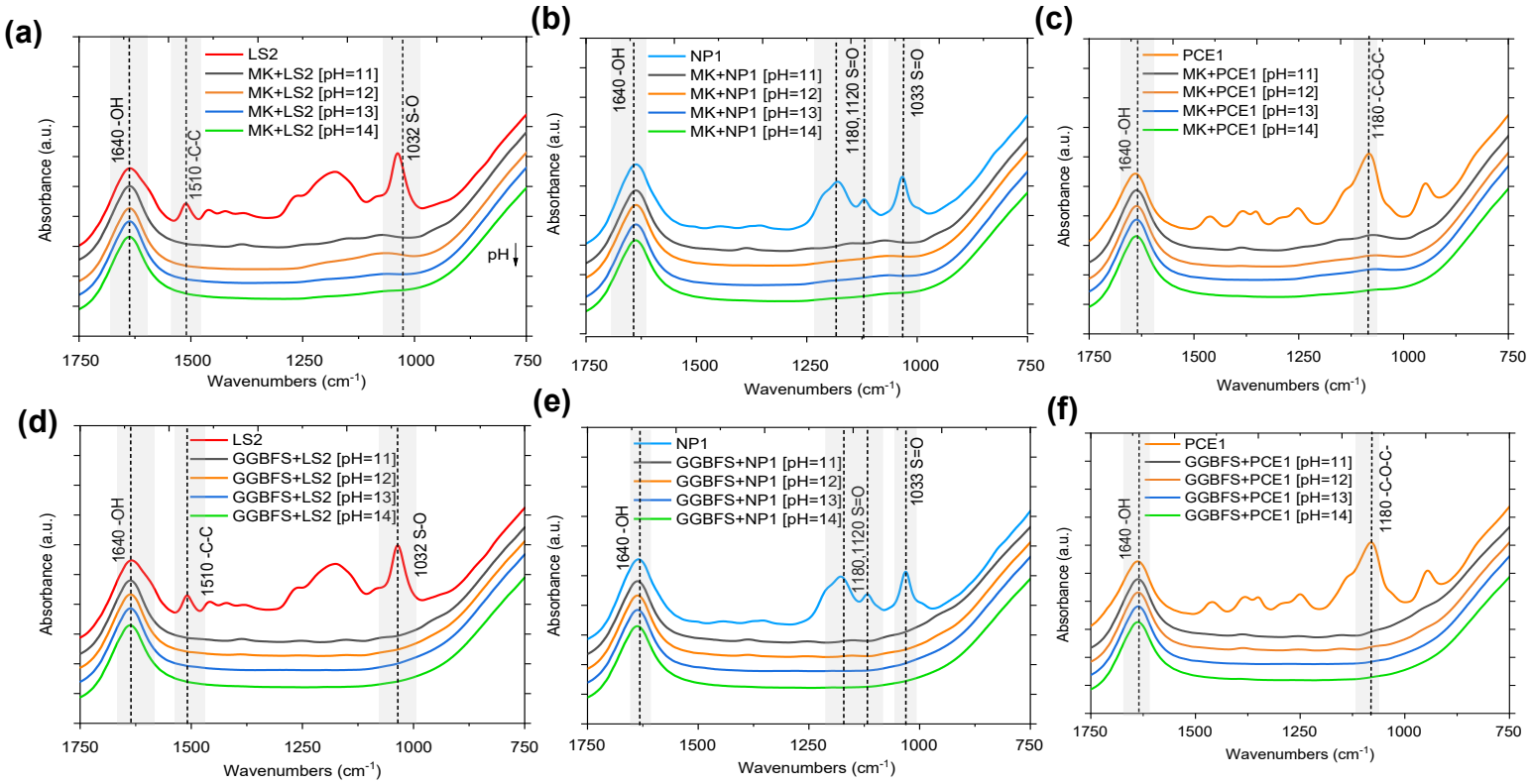

Fig. 5. Liquid ATR-FTIR spectra of the MK and GGBFS suspensions at different pH levels. (a)MK+LS2 (b)MK+NP1 (c)MK+PCE1 (d)GGBFS+LS2 (e)GGBFS+NP1 (f)GGBFS+PCE1.

3.2.2 Effect of pH via DLS

DLS was used to determine the hydrodynamic radius (steric size) of the superplasticiser molecules in the dilute dispersions of the superplasticisers. LS2, NP1, and PCE1 in alkaline solutions, at various pH values (Fig. 6). In DI water (pH 7), a steric size around 40-80 nm, 9nm-20 nm, and 2-3 nm was observed for LS2, NP1, and PCE1, respectively. As the pH increases, the superplasticisers exhibit an apparent particle size distribution comprising larger particles. LS2 seems to be more resistant to pH changes amongst the superplasticisers as increasing the pH from 7 to 14 increased the apparent particle size of LS polymers to a minor extent, compared to NP-based and PCE-based superplasticisers. For example, as the pH increased from 8 to 14, LS2 presented steric size values around 100-200 nm. At this pH interval, NP and PCE had a more pronounced increase in particle size from 10-20 nm to ≥ 4000 nm and from 2.25nm to ≥ 4000nm, respectively. The results suggest agglomeration and/or reduction in solubility of superplasticiser polymers under high alkaline media as one of the causes of their less efficient performance in AAMs. This could explain the reduced performance of superplasticisers in AAMs as observed in the mini-slump test, and corroborate to the changes in the ionisation state of superplasticisers in high alkaline solution, as observed by ATR-FTIR.

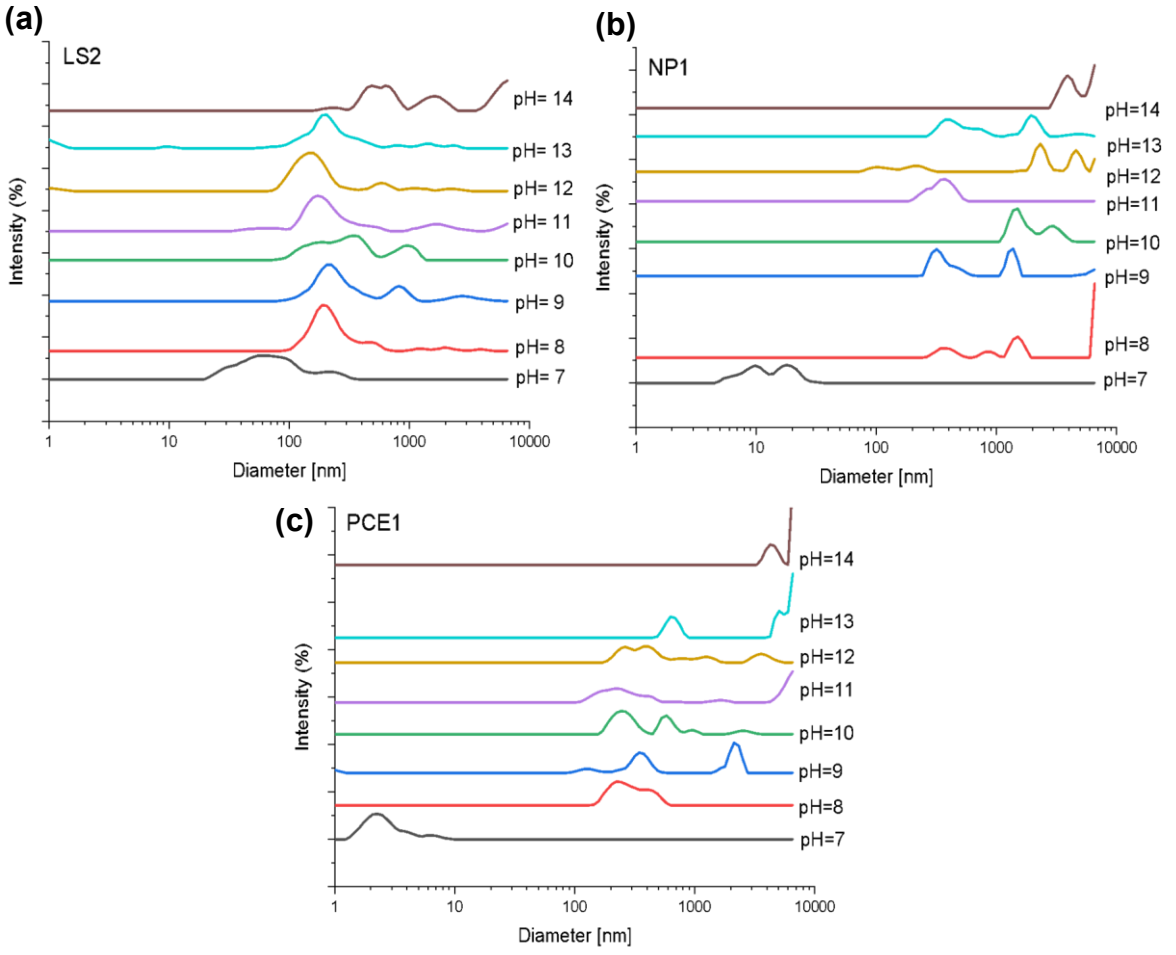

Fig. 6. Particle size distribution of (a) LS2, (b) NP1, and (c) PCE1 at different pH values, as determined by DLS.

Additionally, the DLS results show that the bi-modal shape of some samples becomes even more pronounced as the pH increases. Zhang [33] analysed the chemical stability of LS-, NP-, M-, and PCE-based superplasticisers in different molarities (0.1-10 M of NaOH), and attributed the presence of insoluble solids with different sizes to a high concentration of NaOH causing an alkaline degradation of the superplasticiser molecules into smaller molecules. Similarly, some authors have suggested that PCE side chains degrade in high alkaline media [34,35]. Thus, the polyethene oxides from the side chains of PCEs could interact with ions present in the pore solution and form precipitates of various size distributions. Contrary to that, Chen and Plank [25] recently discussed that PCE polymer does not decompose in activator solutions, regardless of the alkaline concentration or exposure time (1h/1d), instead attributing the observed behaviour to reduced solubility. On the other hand, this study uses commercial superplasticisers, not pure polymers; therefore, it cannot be discarded that some secondary compounds present did not decompose or interact with the alkaline media.

3.2.3 Effects of pH via TEM/EDX

Fig. 7 shows the TEM/EDX results of the superplasticisers in DI water and NaOH solution (1 M, pH=14). In DI water, all the superplasticisers exhibit a greater dispersion. LS2 presented a matrix with dispersed components of different particle sizes. As a LS-based superplasticiser, these components are likely randomly branched polyelectrolyte macromolecules in a lignin structure [10] together with secondary phases present in commercial materials. NP1 and PCE had an apparent better dispersion, but due to the small size distribution of their polymers/components, their polymer could not be seen. Increasing the pH to 14 (equivalent of 1 M NaOH), the images show that chemical admixtures tend to agglomerate, forming particles larger than 10,000 nm (1 μm), corroborating the DLS results.

The observed agglomeration of superplasticisers suggests that they behave differently in the aqueous phase of low-carbon cements such as AAM paste, which is characterised by a much higher ionic strength compared to that of OPC paste. According to Lei, Hirata, and Plank [8], this greater ion concentration partially or completely reduces the solubility of superplasticiser chemical admixtures. Another reason for agglomeration is the changes in the EDL leading to the isoelectric point of the suspensions. At more neutral zeta potential values, the electrostatic

interaction between the polymer and the particle surface is weaker. Consequently, the polymers have reduced mobility and agglomerate. This is further explained in the following section.

The images also show different agglomerates/conformations depending on the type of superplasticiser in highly alkaline media. LS2-based superplasticiser presented more localised sites of agglomerates with circular-shaped appearance, likely due to the more cross-linked and gel-like structure of LS [12]. The EDX data show high concentrations of C, Na, O, Ca, and S ions in the image for the LS2-based superplasticiser, confirming the presence of LS polymer. In highly alkaline media (in NaOH solution, pH = 14), N1 agglomerated in more regions with a rod-like shape morphology. Similar observations were made by Tian et al. [36], who attributed the loss of NP efficiency in AAS to the micelle-like formation of a rod-like shape. Micelles are colloidal agglomerates formed in aqueous solutions by self-assembling amphiphilic copolymers, resulting in a hydrophobic core and hydrophilic shell [37].

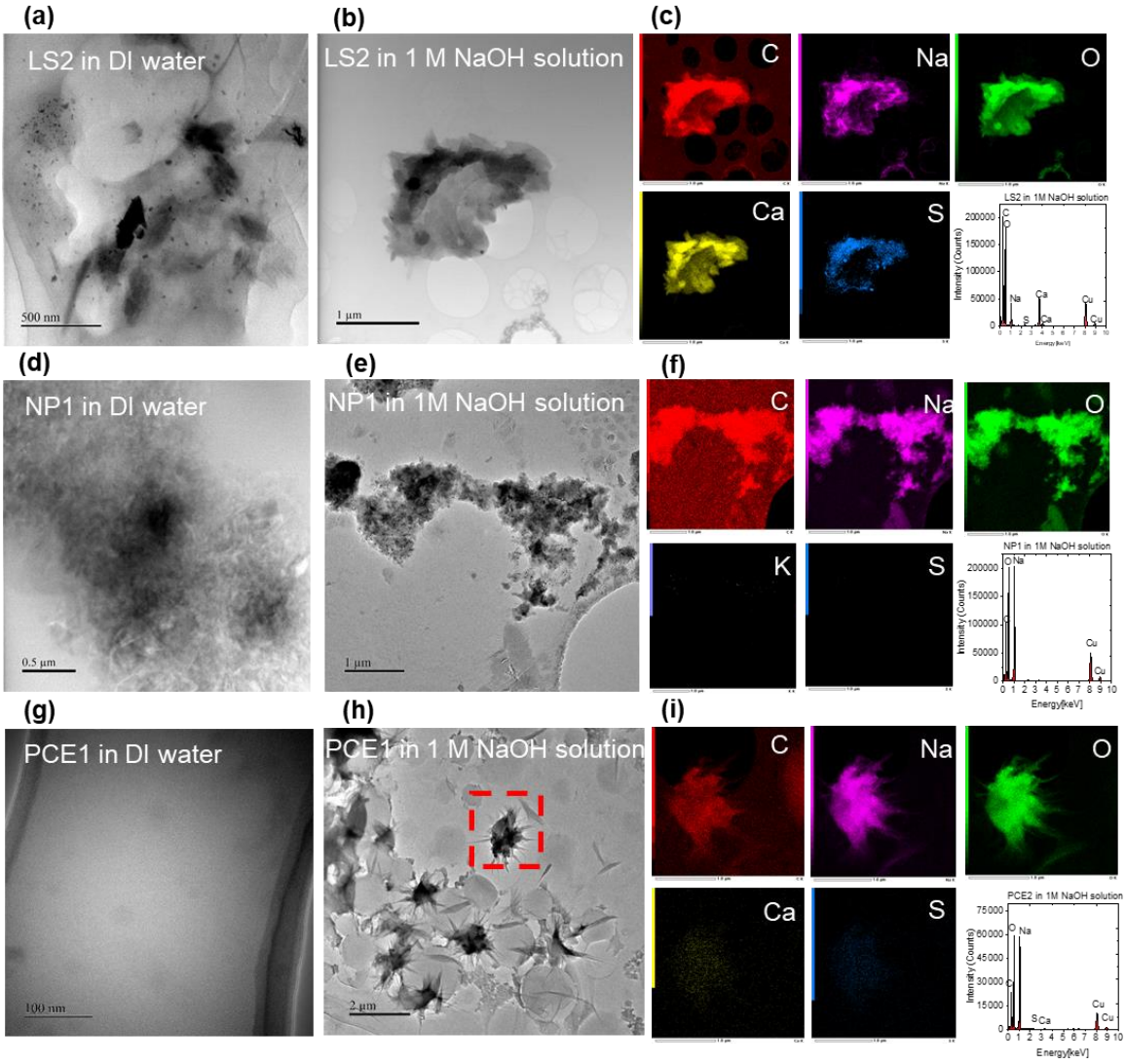

Fig. 7. TEM/EDX images of the superplasticisers in DI water and 1M NaOH solution: (a) LS2 in DI water, (b) LS2 in 1M NaOH solution, (c) Chemical Composition of LS agglomerates, (d) NP1 in DI water (e) NP1 in 1M NaOH solution. (f) Chemical composition of NP1 agglomerates, (g) PCE1 in DI water, (h) PCE1 in 1M NaOH solution, (i) Chemical composition of PCE1 agglomerates.

A more reserved micelle-like formation was predominantly observed for the PCE samples. In highly alkaline media (in NaOH solution, pH = 14), needle-like products were observed covering the PCE micelle-like agglomerates and randomly distributed in the solution. The predominance of Na and O elements in the EDX maps suggests that these products are likely formed from the reaction of NaOH with some PCE compounds, as these needle-like products are not observed in LS- and NP-based superplasticisers. There are two hypotheses to explain the formation of this needle-like product. The PCE side chains, which are less stable in stronger alkaline environments, may break down into smaller molecules, as suggested by Palacios and Puertas [35]. The other option is simply ions interaction of the side chain with sodium (Na^+) and hydroxide ions (OH^-) in the solution, forming crystalline structures. The TEM observations can be linked to the mini-slump results. The more stable to changes polymers, such as LS polymers, would be more resistant to this alkaline environment and promote a better dispersion. On the other hand, NP or PCE polymers going through agglomeration would be a consequence of their reduced availability in solution to interact and adhere to cementitious particles.

Various strategies in polymer design can address the low alkaline resistance and agglomeration in PCE polymers, such as reducing the length of PCE side chains and manipulating backbone stiffness, etc. Studies with different PCE macromonomers have shown that polymer backbones with high molecular weight (M_w) and short side chains had the highest dispersion efficiency in AAS systems [38], which could increase the backbone adsorption and reduce the likelihood of side chains suffering hydrolysis and forming precipitates. However, the chemistry of these macromonomers differently affects their adsorption capacity. Li et al. [39] showed that the HPEG synthesised with poly(methyl methacrylate) (PMMA) acid introduced a methyl group ($-CH_3$) in the polymer backbone. This improves the performance of the backbone by reducing shrinkage, which means that more anchoring groups can be exposed for the adsorption of superplasticisers. On the other hand, a study on MPEG macromonomers reported that PMMA would prevent the penetration of divalent cations (such as Ca^{2+}) and ion condensation [40]. It

563 is worth mentioning that these studies were limited to AAS, and further research is needed for
564 MK-based AAMs.

565 The solubility issues also need further investigation regarding polymer engineering. The use of
566 hydrophilic functional groups, alkali-resistant polymers, and novel PCEs can help mitigate this
567 limitation. However, according to Lei and Chan [38], high solubility does not always mean
568 high dispersion. Most importantly, the polymer needs to be able to reach and adsorb onto the
569 particle surface to promote dispersion.

570 3.3 Adsorption and zeta potential behaviour

571 3.4.1 Zeta potential with varying pH

572 This section shows the effects of pH on the zeta potential charges of suspensions involving MK
573 or GGBFS with varied types of superplasticisers. This brings insights into how varied NaOH
574 concentrations affect the surface interactions in AAMs. Dispersions of MK and GGBFS in the
575 presence of superplasticisers in chemically simplified solutions exhibited zeta potential values
576 dependent on solution pH (Fig. 8), indicating that the pH affects the EDL of MK and GGBFS
577 with superplasticisers. Overall, as the pH increases, the zeta potential of MK and GGBFS
578 becomes less negatively charged. At pH 11, MK exhibited a zeta potential of -104.8 mV (±0.93
579 mV), -59.8 mV (±0.74 mV), -91.2 mV (±0.97 mV), and -95.4 mV (±1.13 mV) for the reference
580 (no superplasticiser), LS1, NP1, and PCE1 samples, respectively. As the pH increases, MK
581 particles dissolve and release mainly Si and Al ions into the solution. The positive nature of
582 these ions leads to a less negative EDL measured in the zeta potential plan, as evidenced in Fig.
583 7. At pH 12, the zeta potential results become less negative, with values of -51.4 mV (±0.68
584 mV), -41.2 mV (±0.93 mV), -64.8 mV (±2.75 mV), ND -41.1 mV (±1.12 mV) for the reference,
585 LS2, NP1, and PCE1 samples, respectively.

586 At pH 13, closer to the pH expected in the pore solution of fresh AAM paste, MK had a zeta
587 potential of -5.4 mV (±2.04 mV), -8.8 mV (±1.78 mV), -7.2 mV (±1.57 mV), -2.4 mV (±1.58
588 mV) for the reference, LS1, NP1, and PCE1 sample, respectively. At this point, LS1 had the
589 more negative zeta potential observed than NP1 and PCE1, likely due to the superplasticisers'
590 molecular structure differences and thereby, by different charge density of the polymers. It is
591 known that LS polymers consist of multiple sulfonate groups ($–SO^{-3}$) distributed along a large,
592 cross-linked and highly anionic structure, which consequently provides more negative sites
593 compared to the other types of superplasticisers (NP1 or PCE1) as measured via zeta potential

test. Therefore, the negative charges provided by the sulfonate groups of NP or comb-like structures of PCEs are not as pronounced as on LS-based superplasticisers.

Increasing the pH to 14, MK exhibited positive zeta potential results of 1.7 mV (±1.31 mV), 5.4 mV (±1.69 mV), 4.8 mV (±1.22 mV), and 3.2 mV (±1.4 mV). The values close to zero from pH 13 to 14 also indicate another potential reason behind the lower effectiveness of superplasticisers in alkaline-activated materials. Between this pH interval, the zeta potential values are likely to reach the isoelectric point, which means the pH at which the surface has no net electrical charge. At this point, the positive and negative charges are balanced (neutral charges), reducing the mobility of superplasticisers' polymers moved by electrostatic forces. Finding high ionic strength, balanced charges and high alkaline media, the superplasticisers do not move, do not adsorb onto the surface particles and therefore agglomerate, corroborating the observations in the DLS data that show increasing particle size distribution as the pH increases.

Due to the presence of Ca^{2+}, GGBFS has a less negatively charged surface than MK. At pH 11, GGBFS exhibited zeta potential values of -74.6 mV (±1.05 mV), -71.4 mV (±0.58 mV), -75.7 mV (±0.82 mV), and -55.4 mV (±1.82 mV) for the reference, LS2, NP1, and PCE1, respectively. As the pH increases, mainly Si, Al, and Ca dissolution starts, impacting the zeta potential results. At pH 12, the values were -48.2 mV (±1.59 mV), -40.7 mV (±1.48 mV), -40.5 mV (±0.75 mV), and -19.2 mV (±2.76 mV) for the reference, LS2, NP1, and PCE1 samples, respectively. Similar to the behaviour of MK suspensions, GGBFs have zeta potential values very close to the isoelectric point. The results at pH 13 were -2 mV (±1.53 mV), -5.7 mV (±2.21), -2.8 mV (±1.9 mV), and 0.8 mV (±1.33 mV) for the reference, LS2, NP1, and PCE1, respectively. Note that the same behaviour of LS2- being more negative than NP1- and PCE1-based superplasticisers was also observed.

At pH 14, the zeta potential values turned positive and the differences between the superplasticisers were negligible. The zeta potential results were 2.4 mV (±1.32 mV), 2.4 mV (±1.46), 4.8 mV (±0.74), and 2.6 mV (±1.41) for LS1, NP1, and PCE1, respectively. These values are close to those found by Chen and Plank [41] testing NaOH-alkali-activated cements with different dosages of superplasticisers (PCE type) (~ +3 mV). The authors reported that zeta potential results indicate that NaOH drastically reduces the PCE adsorption onto the particles' surfaces. At such high alkalinity, the high concentration of Na^{+} in the solution can compress the EDL around the particle surfaces, effectively screening the negative charges of both the particle and the superplasticiser functional groups. This charge screening could be

potentially reducing the electrostatic attraction between superplasticiser molecules and the particle surface, thereby lowering the zeta potential results.

For both MK and GGBFS, the interval between 13 to 14 also marks the isoelectric point of the suspensions, which is defined as the point where the zeta potential charges are neutral. The more neutral zeta potential values, the lower is the electrostatic interaction between the polymer-particle surface. As a result, the polymers are likely to present reduced mobility and, consequently, agglomerate as seen in TEM results. To summarise, increasing the pH drives the dissolution of the precursor materials but simultaneously affects the superplasticisers' surface interactions by resulting in low polymer mobility, agglomeration and low adsorption of superplasticisers to the surface of the solid MK and GGBFS particles.

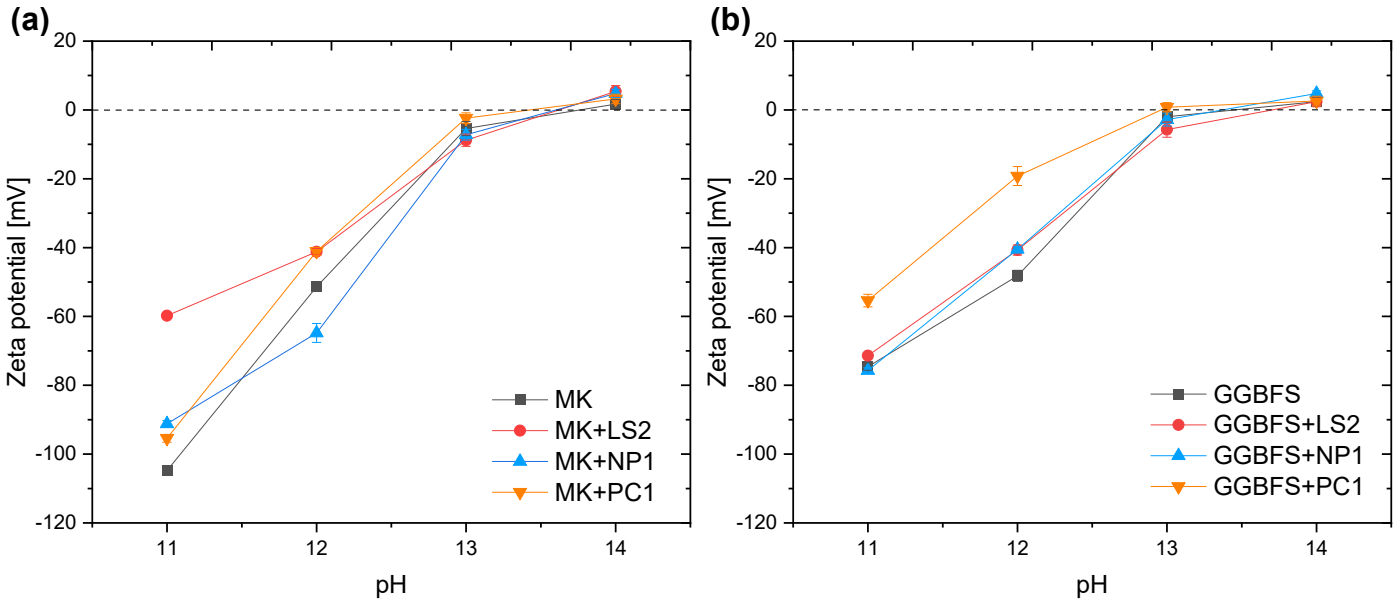

Fig. 8. Zeta potential of MK and GGBFS suspensions at different pH values (11-14). 1% superplasticisers (wt.% of precursor). (a) MK, MK+LS2, +NP1, +PCE1 (b) GGBFS, GGBFS+LS2, +NP1, +PCE1. Results expressed as average value with error bars representing the standard deviation.

3.4.2 Effects of dissolved silica (SiO_2 and Silica fume concentration)

As discussed, the pore solution of AAMs has a high alkalinity and ionic strength. In GGBGS or MK activated by NaOH+Na_2SiO_3, there are multiple ions in the pore solution, such as Si, Al, Na, and Ca. This section reports the influence of Si ions on the zeta potential results, elucidating the role of Si present in the AAMs pore solutions, changing the electrostatic interactions and zeta potential results. Fig. 9 shows the zeta potential values of dispersions of

MK and GGBFS in the presence of superplasticisers in chemically simplified solutions with different Si concentrations (in the form of silica fume or silicon oxide). Compared to the reference ($1x10^{-10}$ M), the addition of Si increased the zeta potential of the suspensions, becoming more positive and reaching the isoelectric point. However, amongst the superplasticiser suspensions, the differences became negligible for both Si-rich materials.

As illustrated in Fig. 9 (a-b), a filler effect of silica oxide (quartz) provides a zeta potential majority in positive values, as it might have enhanced the further dissolution of MK and GGBFS, especially in the presence of superplasticisers. For MK suspensions, the higher average zeta potential results were NP1, PCE1, LS1, and reference (no superplasticisers) with average values from ~0.1 mV to ~2 mV; while GGBFS suspensions presented the most positive values of zeta potential (in average), PCE1, NP1, LS2, and reference samples with ~0 mV to ~ 3.8 mV.

To understand the contribution of reactive Si ions to the zeta potential, silica fume was used. As illustrated in Fig. 9 (c-d), the highly alkaline solution (pH=13) promotes the dissolution of more reactive Si ions into the suspensions, which leads to the zeta potential of MK and GGBFS to less negative values. Overall, there were no significant differences in the zeta potential of MK and GBBFS suspensions with different superplasticisers. For both MK suspensions, NP1 and LS2 showed similar and negative values among the concentrations in the presence of Si, such values around ~ -2 mV and ~ -1 mV for MK and GGBFs, respectively. On the other hand, the effects of Si seemed to be slightly more pronounced in suspensions with PCE, as the zeta potential values were higher than those of other superplasticisers or the reference samples. Rakhimbayev et al. [42] used dynamic modelling simulations and density functional theory calculations to investigate the effects of silica fume on intermolecular interactions between PCE and calcium ions. They concluded that the presence of SiO_2 could improve the PCE adsorption on calcium ions. Thus, in the case of GGBFS, the synergic interaction between Si ions and Ca^{2+} could facilitate the PCE interactions and impact the zeta potential values, which would not happen in MK particles.

The results conclude that Si ions are not the main ions changing the zeta potential of suspensions containing MK or GBBFS in the presence of different superplasticisers. Even though the chemical effects of Si on the superplasticisers' zeta potential seem minor, it is important the study the effect of Si in AAMs. Si-based activators (e.g. sodium silicate) have high viscosity that negatively affects the fluidity of AAM mixes and should be taken into

account when understanding the effects of different phases, reducing the efficiency of superplasticisers [9].

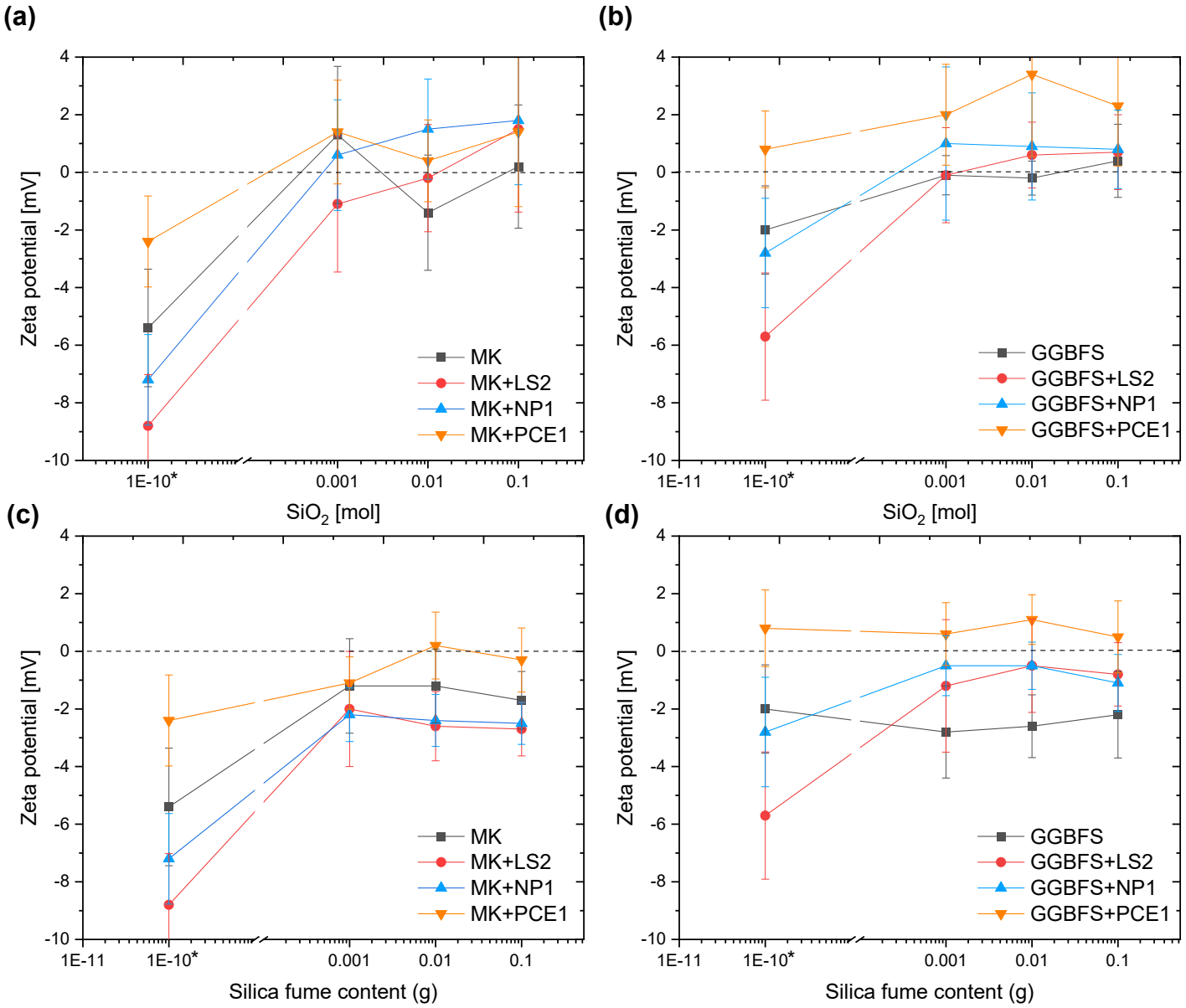

Fig. 9. Zeta potential of MK and GGBFS suspensions at different SiO_2 concentrations (0.001-0.1) and silica fume contents (0.001, 0.01, 0.1). (a,c)MK, MK+LS2, +NP1, +PCE1 (b,d) GGBFS, GGBFS+LS2, +NP1, +PCE1. 1% superplasticisers (wt.% of precursor). *considered as reference (no SiO_2 or silica fume). pH =13. Results expressed as average value with error bars representing the standard deviation.

3.4 Influence of sodium ions (NaCl concentration)

This section shows the influence of Na ions on the zeta potential results, elucidating the role of Na present in the AAMs pore solutions changing the electrostatic interactions and zeta potential results. Note that the existing Na from NaOH is not considered into the total Na ion concentration. Fig. 10 shows the zeta potential values of dispersions of MK and GGBFS in the presence of superplasticisers in chemically simplified solutions with different NaCl concentrations. Three main mechanisms can be proposed to explain the interactions of Na with the MMK and GGBFS particle suspensions. When added to the alkaline solution (pH=13), NaCl dissociates into Na^+ and Cl^- monovalent ions. Na^+ ions attract and neutralise some negative charges in the alkali solution, resulting in a less negative zeta potential. Additionally, there is the adsorption of Na^+ on the superplasticisers' functional groups, which can be the sulfonated groups of LS and NP, or side chains for PCE superplasticisers. Predictably, fewer negative sites for Na adsorption are present in the superplasticisers when these interactions happen. The third interaction will be with the particles. These ions will interact with the dissolving surface of MK and GGBFS and Change the zeta potential charges.

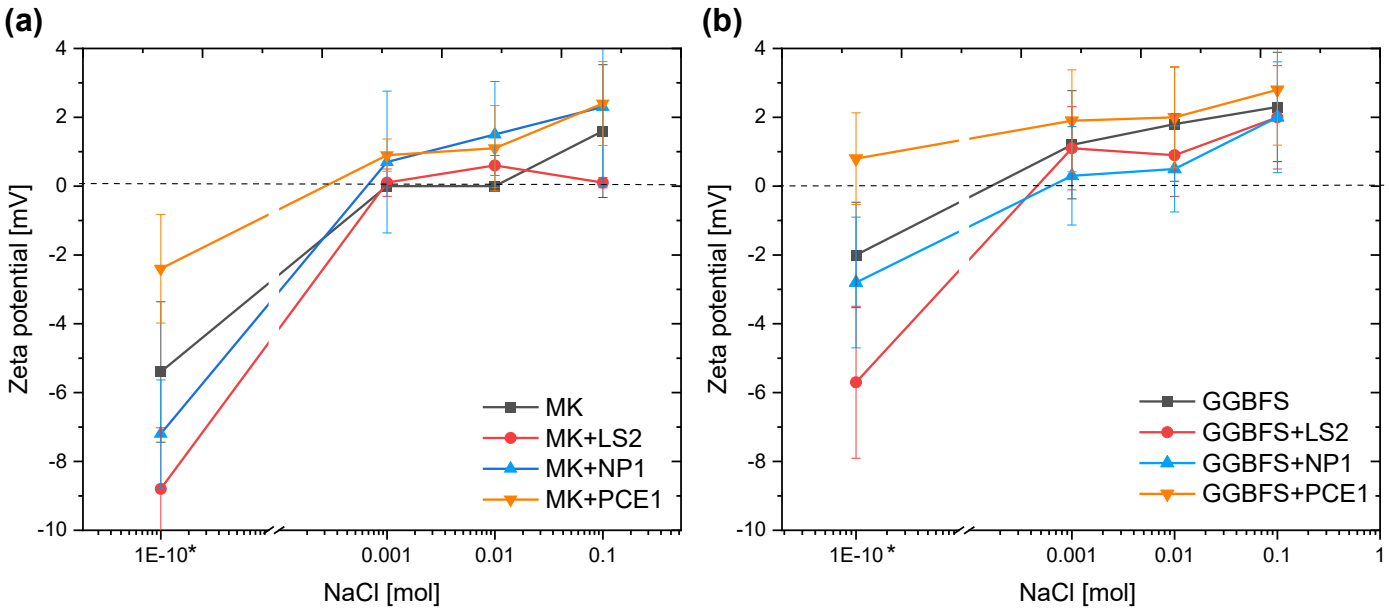

Fig. 10. Zeta potential of MK and GGBFS suspensions at different NaCl concentrations (0.001-0.1). (a) MK, MK+LS2, +NP1, +PCE1 (b) GGBFS, GGBFS+LS2, +NP1, +PCE1. 1% superplasticisers (wt.% of precursor). *considered as reference (no NaCl). pH =13. Results expressed as average value with error bars representing the standard deviation.

For MK suspensions, NP and PCE probably have fewer negative sites to interact with Na cations and MK surfaces than LS, which might explain the lower zeta potential values compared to GGBFS. When NaCl is added to the GGBFS solutions, higher zeta potential results are observed, which is influenced by the more positive surface of the slag. The presence of Ca from GGBFS reduces the zeta potential when NP1 is used. In both suspensions, PCE-superplasticisers seemed to have more coherent interactions leading to positive zeta potential values.

3.5 Influence of Ca ions ($CaCl_2$ concentration) and adsorption

This section presents the influence of Ca ions on the zeta potential results, elucidating the role of Ca present in the AAMs pore solutions, changing the electrostatic interactions and zeta potential results. Additionally, the addition of Ca ions as a strategy to improve superplasticiser adsorption on the MK or GGBFS particles was assessed. Fig. 11 shows the zeta potential values of dispersions of MK and GGBFS in the presence of superplasticisers in chemically simplified solutions with different $CaCl_2$ concentrations. The divalent cations (Ca^{2+}) present in these solutions modify the EDL following the same principle as Na^{+}, i.e., neutralising some negative charges, interacting with some anchor groups for the superplasticisers, and adsorbing on the particles' surface. Consequently, the addition of $CaCl_2$ resulted in a less negative zeta potential for all concentrations. The results of zeta potential were from approximately -10 mV (0.001 M of $CaCl_2$) to +2 mV (0.1 M of $CaCl_2$) amongst the suspensions of both MK and GGBFS. For MK, the increasing addition of $CaCl_2$ appears to have a greater effect on the zeta potential of PCE1 compared to the reference (MK), LS2, and NP1-based superplasticisers, respectively. For GGBFS, such an effect appeared to be more similar among the suspensions but slightly higher for PCE1, reference, NP1, and LS2, respectively. The results suggest a better interaction

between PCE and calcium as the systems get closer to a high-calcium system, such as in OPC systems.

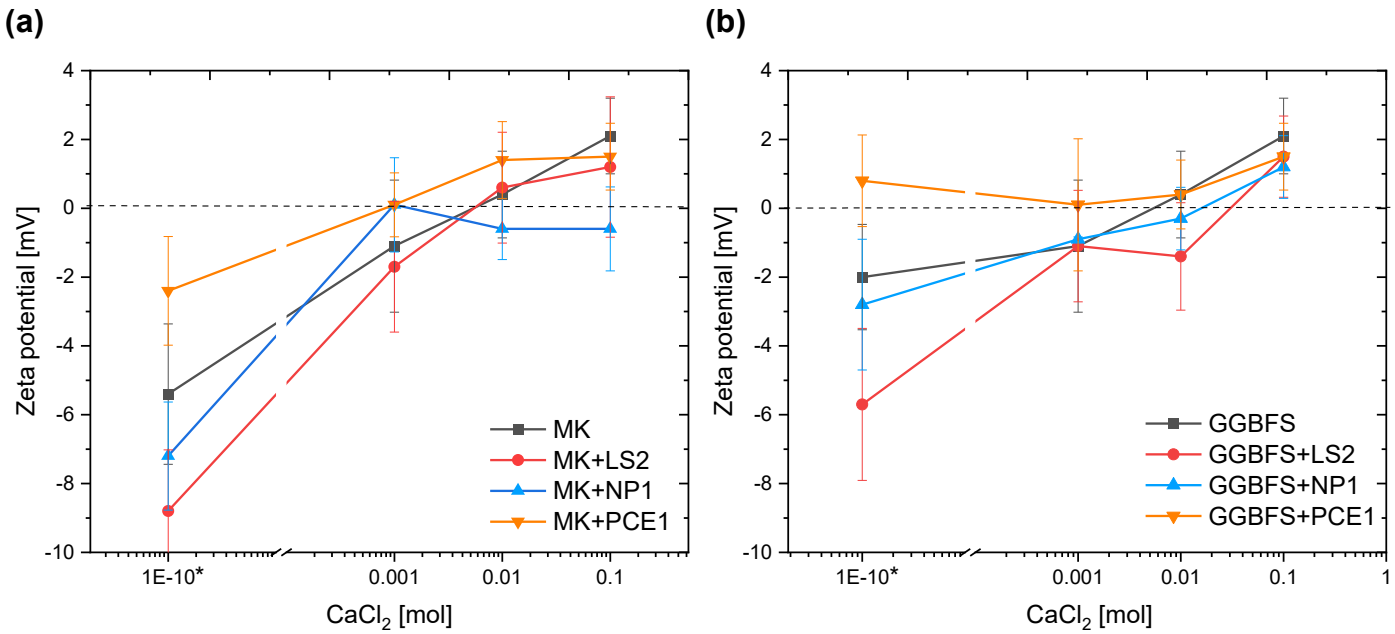

Fig. 11. Zeta potential of MK and GGBFS suspensions at different $CaCl_2$ concentrations (0.001-0.1). (a)MK, MK+LS2, +NP1, +PCE1 (b) GGBFS, GGBFS+LS2, +NP1, +PCE1. 1% superplasticisers (wt.% of precursor). *considered as reference (no $CaCl_2$). pH =13. Results expressed as average value with error bars representing the standard deviation.

Fig. 12 shows the TOC results of MK and GGBBFS suspensions with superplasticisers in the presence of $CaCl_2$. As expected, adding $CaCl_2$ also increased the adsorption of the superplasticisers on MK and GGBFS particles in NaOH solution (pH=13). It is well-known that the role of Ca^{2+} ions facilitates the adsorption of superplasticisers on the particle surfaces of different cementitious materials. These ions convert the negatively charged surface of various particles into less negative or positively charged surfaces and work as bridge sites for the adsorption of anionic dispersants, producing a Langmuir-type adsorption isotherm [43]. MK shows synergy with superplasticisers because its highly negative surface interacts with Ca^{2+} ions, which in turn promote polymer adsorption. Without $CaCl_2$ (e.g. superplasticiser+MK), MK already adsorbs most of the polymers (88% LS2, 72% NP1, 93% PCE1) through direct electrostatic attraction. When $CaCl_2$ is added, the extra Ca^{2+} ions create cation-bridging between MK and the anionic groups of the polymers, increasing adsorption to

92-100% for LS2, 93-100% for NP1, and 99-100% for PCE. This explains the more pronounced effect observed in MK.

It is important to note that changes in EDL induced by $CaCl_2$ concentrations, as measured by zeta potential, do not necessarily indicate a higher adsorption capacity of superplasticisers on the particles. While zeta potential analysis measures the surface charges around the EDL, the mechanisms driving these interactions are more complex. The observation that LS-based superplasticisers achieved 100% adsorption on GGBFS particles for all samples, compared to adsorption of 39%-42% for NP and 25-27% for PCE-based superplasticisers, supports the idea that not all Ca^{2+} ions in the pore solution measured by zeta potential act as anchoring sites for superplasticisers adsorption as it would be expected similar behaviour amongst the samples or high adsorption capacity when PCE is used. To a lesser extent, there might be effects of Cl^- on the zeta potential and TOC results. The Cl^- ions can increase the overall ionic strength of the solution, modify the zeta potential values, leading to more negative values, and interact with surface sites and influencing how much Ca^{2+} can be adsorbed.

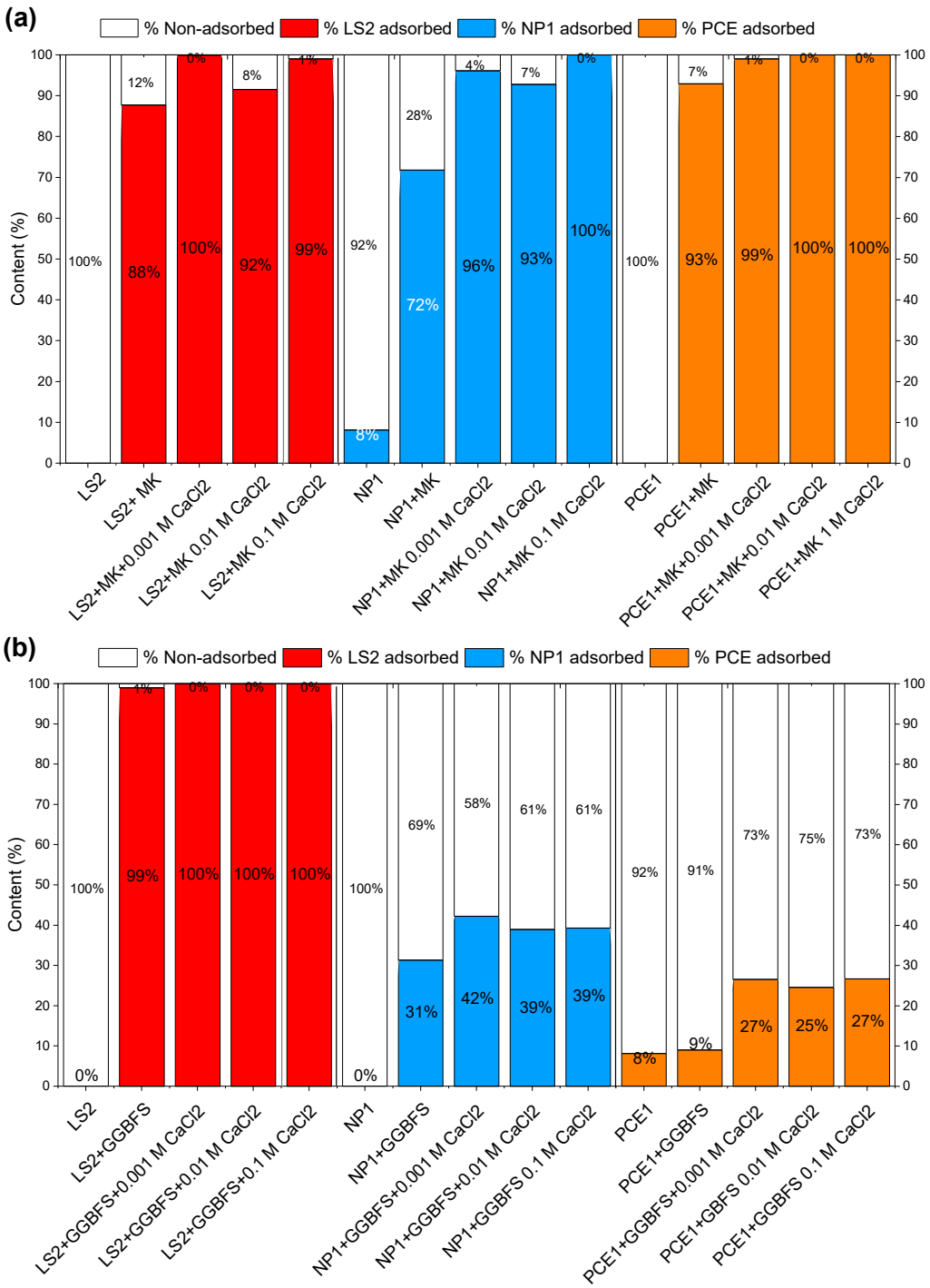

Fig. 12. TOC data of MK and GGBFS suspensions in NaOH solution with superplasticisers at different $CaCl_2$ concentrations (0.001 M-0.1 M), obtained by depletion method (a) LS2, NP1, PCE1, MK+LS2, MK+NP1, MK+PCE1 (b) LS2, NP1, PCE1, GGBFS+LS2, GGBFS+NP1, GGBFS+PCE1. 1% superplasticisers (wt.% of precursor).

4 Proposed mechanism of particle-surface interaction

The interaction mechanism between MK or GGBFS particles and various superplasticiser types in AAM-relevant solutions plays an important role in determining the dispersion and fluidity of AAM pastes. The mini-slump tests showed divergences in the performance of superplasticisers in both AAMs based on MK or GGBFS, showing the complexity of these systems and limitations of traditional PCE-based superplasticisers that normally have a better performance at low dosages in OPC-systems.

Fig. 13 illustrates the proposed mechanisms of interaction of the surface of the solid GGBFs or MK particles and the LS-, NP-, and PCE-based commercial superplasticisers in AAM-relevant solutions. AAMs are inherently more alkaline than PC systems due to the use of alkali activators (e.g. NaOH or Na_2SiO_3). When LS, NP or PCE-based superplasticisers are added to these solutions, they immediately experience a highly alkaline media, with high ionic strength and high concentration of Na^+, Si^-, OH^- ions, etc. The high pH (>13) is beneficial to promote the dissolution of the precursors, but it leads to changes in the ionisation states of polymers and the EDL, as shown by ATR-FTIR and zeta potential results. The increase of pH leads to an isoelectric point where the surface charges are neutral (zeta potential ~ 0 mV). This reduces the electrostatic attractions between the particles, promoting the reduced mobility of the superplasticiser polymers with subsequent reduced solubility and agglomeration. NP- exhibited a more rod-like agglomeration, while for PCE-based superplasticisers, micelle-like agglomerates and needle-like precipitates were observed, suggesting that strong alkalis can cleave or interact with side chains and alter polymer architecture, suppressing their adsorption and dispersion ability, especially in MK-based AAMs.

The LS-based superplasticiser is a more stable molecule in the alkaline media. DLS and TEM results showed fewer changes in the apparent steric size and polymer conformation are observed. The cross-linked and gel-like structure of LS polymer resists alkaline degradation and agglomeration, and the potential high charge density of sulfonate groups improves electrostatic compatibility with Na or Ca present at the EDL. AAMK normally requires higher dosages of activators to dissolve Al and Si to form MK framework gel, resulting in a more aggressive chemical environment than GGBFS. Thus, LS-based superplasticisers are preferred due to its high dispersion ability, resistance, and adsorption. Moreover, the presence of residual sugars and lignin compounds contributes to retardation effects, enhancing slump-retention.

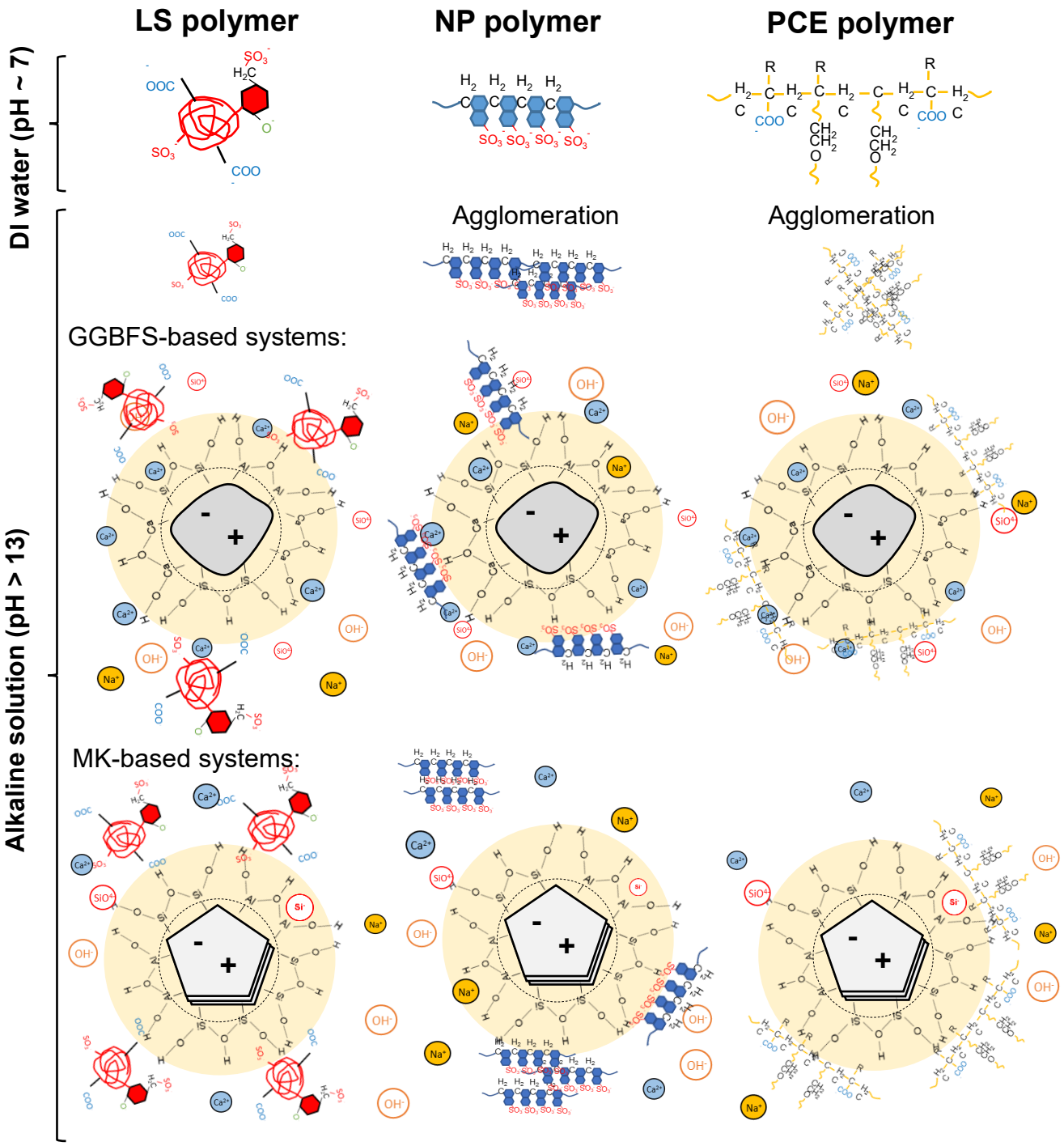

798

799 **Fig. 13.** Schematic representation of the proposed interaction mechanisms between
800 MK/GGBFS particles and polymers of varied superplasticisers in AAMs. The effects of other
801 compounds present in the commercial superplasticisers have not been illustrated (salts,
802 additives, etc.).

803

The different chemical composition of GGBFS, especially related to the presence of calcium, results in distinct surface chemistry and zeta potential behaviour. Ca^{2+} ions present on the EDL shifted the zeta potential values to less negative values independently of the pH or concentration of Si, Na, or additional Ca ions. On the other hand, the presence of Ca in GGBFS does not provide a stronger Ca^{2+} adsorption than MK, according to TOC results.

At high pH (>13), where the surface charges are close to the isoelectric point, Si, Na or Ca ions had minimal or negligible effects on the surface charge. Soluble silica, whether from the dissolution of MK/GBBFS particles or silica fume, as well as from SiO_2, interacted in suspension but minimally modulated the zeta potential. While these materials release Si anions to the solution (e.g., SiO_4^{4-}, $SiO_2(OH)_2^{2-}$), suggesting changes of zeta potential to more negative values are expected, the opposite behaviour was observed. The hypothesis is that these Si ions interact with positive ions such as Na^+ and/or Ca^{2+} to form complexes. These anions are more likely to explain any changes in zeta potential to less negative values. To some extent, they bridge the adsorption of negative functional groups of superplasticisers, which was also higher in LS-based superplasticisers.

5 Limitations and implications for low-carbon cements

Modern concrete production relies on chemical admixtures to improve both fresh- and hardened-state properties. Among these, superplasticisers play a crucial role in increasing workability, enabling higher productivity, and supporting the widespread adoption of low-carbon concrete technologies. To reduce CO_2 emissions from PC production, the industry is increasingly adopting alternative approaches, including the use of waste materials as SCMs, reducing the clinker content, and exploring alternative binders such as AAM, limestone calcined clay cement (LC^3), and (belite)-calcium sulfoaluminate cements (BCSA), etc. However, these approaches introduce new challenges for the superplasticiser design and more fundamental research in this field is needed.

In particular, the effectiveness of traditional superplasticisers can be compromised by the complex chemistry of alternative systems. The presence of this variety of SCMs in alkaline environments alters the pore solution chemistry, which can impact the performance of superplasticisers. Understanding the interaction mechanisms between superplasticisers and SCMs in a range of different conditions is key to addressing issues such as changes in EDL,

834 the factors behind the reduced performance, and the behaviour of certain superplasticiser
835 molecules in high-alkaline media. This highlights the need for developing novel, alkali-
836 resistant superplasticisers tailored to emerging low-carbon cement systems.

837 This study has been limited to the analysis of two typical precursor materials and the scope of
838 three different types of superplasticisers. The results presented can be used to explain the
839 reduced performance of superplasticisers in alkali-activated cements, PC-SCM blends based
840 on GGBFS and MK, and other cements incorporating GGBFS and MK. We suggest future
841 analyses in varied pore solutions chemistry relevant to different types of alternative binders
842 (AAM-relevant, BCSA, and other novel cements) as an attempt to predict material
843 compatibility and performance under more types of SCM, electrolytes, and varied dosages of
844 superplasticisers. There is also a need for investigation of the impact of PCE molecular
845 architecture on the interactions of PCE with varied types of calcined clays and slag materials.
846 Further research exploring nano- and microstructural development of low-carbon cement
847 pastes *in situ* during reaction and setting can yield new information regarding the effects of the
848 reaction mechanisms and kinetics on the dispersive performance of superplasticisers. The use
849 of dynamic modelling of superplasticiser polymers in more realistic ionic environments can be
850 a valuable tool to understand the superplasticiser-particle interactions at the atomic level.
851 Together, this will yield further new insight that is important for the development of the next
852 generation of superplasticisers tailored for alternative cement systems.

853 ## 6 Conclusions

854 The results presented here show that the behaviour of superplasticisers in alkali-activated
855 systems based on GGBFS or MK with Na_2SiO_3+NaOH is as follows:

856 - Higher pH values result in greater dissolution of the solid precursors and reduced
857 superplasticiser stability as the pH changes the ionisation state of superplasticisers in
858 solution.
859 - When the superplasticisers are added to the alkaline solutions, their components
860 undergo partial degradation and polymer agglomeration, explaining the
861 superplasticisers' larger apparent particle size distribution. This phenomenon is more
862 pronounced in PCE and NP-based samples than in LS, which can be related to polymer
863 resistance and higher solubility in alkaline solutions.

- Agglomeration of LS seems to be more spherical in morphology, which is in line with the more circular/branched-like shape of LS polymers, NP in the conformation of rod-like micelles, and PCE in the forms of more circular micelles with needle-like structures on their surface.
- Electrolytes affect the EDL of GGBFS and MK particles differently. Si ions were shown to have a negligible effect while Na and Ca ions had positive effects in creating bridge sites to facilitate the adsorption of superplasticisers.
- The adsorption of LS based on the GGBFS and MK surface particles was facilitated by the addition of $CaCl_2$ (which provided Ca^{2+} ions) compared to NP- and PCE-based superplasticisers.
- The nature of LS-based superplasticisers promotes higher stability, lesser agglomeration, better Ca^{2+} adsorption and better fluidity.

The results presented here provide new insight into the different behaviour of the most typical superplasticisers used in modern concrete formulations, for applications in AAMs based on GGBFs or MK. The strategies for the upcoming generation of chemical admixtures should focus on developing high-resistance polymers in hostile media, with high solubility. The characteristics of LS-based superplasticisers can help design the next generation of superplasticisers for AAM systems. Some of these features could be added to the versatile PCE synthesis to improve performance in high pH cement systems.

Declaration of Competing Interests

The authors declare that they have no known competing financial interests or personal relationships that could have appeared to influence the work reported in this paper.

Data availability

Most data can be found in the Supplementary Material. Any further data will be made available on request.

Acknowledgements

The participation of MRCS was sponsored by a PhD scholarship (Studentship 2735216) from the Engineering and Physical Sciences Research Council (EPSRC), UK, administered through the Energy Institute, The University of Sheffield. CNPq sponsored APK through the research fellowship 311893/2021-0. The author acknowledges CNPq for the grant 444612/2024-6, who promote international cooperation. The authors would like to thank SIKA and Chryso Saint-

Gobain for the provision of the superplasticisers, and Professor Johann Plank, Technical University of Munich, for insightful discussion related to this work.

References

[1] R. Flatt, I. Schober, Superplasticizers and the rheology of concrete, in: Underst. Rheol. Concr., Elsevier, 2012: pp. 144–208. https://doi.org/10.1533/9780857095282.2.144.

[2] J.L. Provis, Alkali-activated materials, Cem. Concr. Res. (2018). https://doi.org/10.1016/j.cemconres.2017.02.009.

[3] J.L. Provis, S.A. Bernal, Geopolymers and Related Alkali-Activated Materials, Https://Doi.Org/10.1146/Annurev-Matsci-070813-113515 44 (2014) 299–327. https://doi.org/10.1146/ANNUREV-MATSCI-070813-113515.

[4] A. Habbaba, J. Plank, Surface chemistry of ground granulated blast furnace slag in cement pore solution and its impact on the effectiveness of polycarboxylate superplasticizers, J. Am. Ceram. Soc. 95 (2012) 768–775. https://doi.org/10.1111/j.1551-2916.2011.04968.x.

[5] M.H. Derkani, N.J. Bartlett, G. Koma, L.A. Carter, D.A. Geddes, J.L. Provis, B. Walkley, Mechanisms of dispersion of metakaolin particles via adsorption of sodium naphthalene sulfonate formaldehyde polymer, J. Colloid Interface Sci. 628 (2022) 745–757. https://doi.org/10.1016/J.JCIS.2022.07.166.

[6] B.M. Mercado-Borrayo, R. Schouwenaars, J.L. González-Chávez, R.M. Ramírez-Zamora, Multi-analytical assessment of iron and steel slag characteristics to estimate the removal of metalloids from contaminated water, J. Environ. Sci. Heal. - Part A Toxic/Hazardous Subst. Environ. Eng. 48 (2013) 887–895. https://doi.org/10.1080/10934529.2013.761492.

[7] E.U.S.U. Nägele, The zeta-potential of blast furnace slag and fly ash, Cem. Concr. Res. 19 (1989) 811–820.

[8] L. Lei, T. Hirata, J. Plank, 40 years of PCE superplasticizers - History, current state-of-the-art and an outlook, Cem. Concr. Res. 157 (2022) 106826. https://doi.org/10.1016/J.CEMCONRES.2022.106826.

[9] X. Liu, S. Li, Y. Ding, Z. Lu, D. Stephan, Y. Chen, Z. Wang, S. Cui, Investigation on admixtures applied to alkali-activated materials: A review, J. Build. Eng. 64 (2023). https://doi.org/10.1016/j.jobe.2022.105694.

[10] N. Vanitha, T. Revathi, R. Jeyalakshmi, Influence on Rheology and Microstructure of Nanosilica and Modified Polycarboxylate in Water-Glass-Activated Fly Ash/Ground Granulated Blast Furnace Slag Geopolymers, ChemistrySelect 8 (2023) e202203491. https://doi.org/10.1002/SLCT.202203491.

[11] B.O. Myrvold, A new model for the structure of lignosulphonates. Part 1. Behaviour in dilute solutions, Ind. Crops Prod. 27 (2008) 214–219. https://doi.org/10.1016/j.indcrop.2007.07.010.

[12] J. Liu, X. Li, M. Li, Y. Zheng, Lignin biorefinery: Lignin source, isolation, characterization, and bioconversion, Adv. Bioenergy 7 (2022) 211–270. https://doi.org/10.1016/BS.AIBE.2022.05.004.

[13] G. Gelardi, S. Mantellato, D. Marchon, M. Palacios, A.B. Eberhardt, R.J. Flatt, Chemistry of chemical admixtures, in: Sci. Technol. Concr. Admixtures, Elsevier Inc., 2016: pp. 149–218. https://doi.org/10.1016/B978-0-08-100693-1.00009-6.

[14] B. EL HILAL, M.H. Khudhair, A. El Harfi, Review on different families of polymeric superplasticizers used as adjuvants in the cementitious materials in civil engineering, Appl. J. Environ. Eng. Sci. 4 (2018) 4-2(2018) 158-170. https://revues.imist.ma/index.php/AJEES/article/view/11727 (accessed April 7, 2023).

[15] S. Pieh, Polymere Dispergiermittel I. Molmasse und Dispergierwirkung der Melamin- und Naphthalin-Sulfonsäure-Formaldehyd-Polykondensate, Die Angew. Makromol. Chemie 154 (1987) 145–159. https://doi.org/10.1002/APMC.1987.051540111.

[16] Li, W.-C. Chen, L. Lei, J. Plank, Dispersing Efficacy of Tailored IPEG PCEs in AAS Binders: Elucidating the Impact of PCE Molecular Weight, Ind. Eng. Chem. Res. (2023) 12. https://doi.org/10.1021/acs.iecr.2c03820.

[17] L. Kalina, V. Bílek, P. Hrubý, V. Iliushchenko, M. Kalina, J. Smilek, On the action mechanism of lignosulfonate plasticizer in alkali-activated slag-based system, Cem. Concr. Res. 157 (2022) 106822. https://doi.org/10.1016/J.CEMCONRES.2022.106822.

954 [18] M.J. de Hita, M. Criado, Influence of the Fly Ash Content on the Fresh and Hardened
955 Properties of Alkali-Activated Slag Pastes with Admixtures, Mater. 2022, Vol. 15,
956 Page 992 15 (2022) 992. https://doi.org/10.3390/MA15030992.

957 [19] E. Paul, Influence of superplasticizer on workability and strength of ambient cured
958 alkali activated mortar, Clean. Mater. 6 (2022) 100152.
959 https://doi.org/10.1016/J.CLEMA.2022.100152.

960 [20] G. Xiong, X. Guo, Effects and mechanism of superplasticizers and precursor
961 proportions on the fresh properties of fly ash – slag powder based geopolymers,
962 Constr. Build. Mater. 350 (2022) 128734.
963 https://doi.org/10.1016/J.CONBUILDMAT.2022.128734.

964 [21] C. Wang, O. Kayali, J.L. Liow, U. Troitzsch, Participation and disturbance of
965 superplasticisers in early-stage reaction of class F fly ash-based geopolymer, Constr.
966 Build. Mater. 403 (2023) 133176.
967 https://doi.org/10.1016/J.CONBUILDMAT.2023.133176.

968 [22] V. Bílek, L. Kalina, R. Novotný, Structural build-up and breakdown of alkali-activated
969 slag pastes with different order of lignosulfonate and activator addition, Constr. Build.
970 Mater. 386 (2023) 131557. https://doi.org/10.1016/J.CONBUILDMAT.2023.131557.

971 [23] J. Xie, O. Kayali, Effect of superplasticiser on workability enhancement of Class F and
972 Class C fly ash-based geopolymers, Constr. Build. Mater. 122 (2016) 36–42.
973 https://doi.org/10.1016/J.CONBUILDMAT.2016.06.067.

974 [24] T. Luukkonen, Z. Abdollahnejad, K. Ohenoja, P. Kinnunen, M. Illikainen, Suitability
975 of commercial superplasticizers for one-part alkali-activated blast-furnace slag mortar,
976 J. Sustain. Cem. Mater. 8 (2019) 244–257.
977 https://doi.org/10.1080/21650373.2019.1625827.

978 [25] J. Chen, J. Plank, Which factors impact the effectiveness of PCEs in alkali-activated
979 slag cements?, Cem. Concr. Res. 190 (2025) 107807.
980 https://doi.org/10.1016/J.CEMCONRES.2025.107807.

981 [26] G. Lai, Research on synthesis and properties of amphoteric early strength
982 polycarboxylate superplasticizer, IOP Conf. Ser. Mater. Sci. Eng. 631 (2019) 022056.
983 https://doi.org/10.1088/1757-899X/631/2/022056.

[27] D. Zhang, X. Sun, Efficiencies of Super-Plasticizer on Rheology Properties of Fly Ash-Based Alkali-Activated Materials with Different Ms Waterglass Activators, Polym. 2023, Vol. 15, Page 2054 15 (2023) 2054. https://doi.org/10.3390/POLYM15092054.

[28] D.A. Geddes, B. Walkley, C. Le Galliard, M. Hayes, S.A. Bernal, J.L. Provis, Effect of exposure of metakaolin-based geopolymer cements to gamma radiation, J. Am. Ceram. Soc. 107 (2024) 4621–4630. https://doi.org/10.1111/JACE.19747;JOURNAL:JOURNAL:15512916;WGROUP:STRING:PUBLICATION.

[29] J.L. Provis, K. Arbi, S.A. Bernal, D. Bondar, A. Buchwald, A. Castel, S. Chithiraputhiran, M. Cyr, A. Dehghan, K. Dombrowski-Daube, A. Dubey, V. Ducman, G.J.G. Gluth, S. Nanukuttan, K. Peterson, F. Puertas, A. van Riessen, M. Torres-Carrasco, G. Ye, Y. Zuo, RILEM TC 247-DTA round robin test: mix design and reproducibility of compressive strength of alkali-activated concretes, Mater. Struct. Constr. 52 (2019) 1–13. https://doi.org/10.1617/S11527-019-1396-Z/FIGURES/6.

[30] P. Wedding, D. Kantro, Influence of Water-Reducing Admixtures on Properties of Cement Paste—A Miniature Slump Test, Cem. Concr. Aggregates 2 (1980) 95. https://doi.org/10.1520/cca10190j.

[31] M. Hunger, H.J.H. Brouwers, Flow analysis of water-powder mixtures: Application to specific surface area and shape factor, Cem. Concr. Compos. 31 (2009) 39–59. https://doi.org/10.1016/j.cemconcomp.2008.09.010.

[32] J. Plank, B. Sachsenhauser, J. de Reese, Experimental determination of the thermodynamic parameters affecting the adsorption behaviour and dispersion effectiveness of PCE superplasticizers, Cem. Concr. Res. 40 (2010) 699–709. https://doi.org/10.1016/J.CEMCONRES.2009.12.002.

[33] D.W. Zhang, X.M. Sun, Z.Y. Xu, C.L. Xia, H. Li, Stability of superplasticizer on NaOH activators and influence on the rheology of alkali-activated fly ash fresh pastes, Constr. Build. Mater. 341 (2022) 127864. https://doi.org/10.1016/J.CONBUILDMAT.2022.127864.

[34] S. Partschefeld, A. Tutal, T. Halmanseder, J. Schneider, A. Osburg, Investigations on

Stability of Polycarboxylate Superplasticizers in Alkaline Activators for Geopolymer Binders, Mater. 2023, Vol. 16, Page 5369 16 (2023) 5369. https://doi.org/10.3390/MA16155369.

[35] M. Palacios, F. Puertas, Effect of superplasticizer and shrinkage-reducing admixtures on alkali-activated slag pastes and mortars, Cem. Concr. Res. 35 (2005) 1358–1367. https://doi.org/10.1016/J.CEMCONRES.2004.10.014.

[36] Y. Tian, Q. Yuan, C. Yang, K. Yang, L. Yu, M. Zhang, X. Zhu, Insights into the efficiency loss of naphthalene superplasticizer in alkali-activated slag pastes, J. Build. Eng. 68 (2023). https://doi.org/10.1016/j.jobe.2023.106176.

[37] S. Fatima, S.N. Quadri, S. Parveen, S. Beg, M. Rahman, F.J. Ahmad, M.Z. Abdin, Polymeric nanoparticles for potential drug delivery applications in cancer, Nanoformulation Strateg. Cancer Treat. (2020) 65–88. https://doi.org/10.1016/B978-0-12-821095-6.00009-4.

[38] L. Lei, H.K. Chan, Investigation into the molecular design and plasticizing effectiveness of HPEG-based polycarboxylate superplasticizers in alkali-activated slag, Cem. Concr. Res. 136 (2020). https://doi.org/10.1016/J.CEMCONRES.2020.106150.

[39] R. Li, W. Eisenreich, L. Lei, J. Plank, Low Carbon Alkali-Activated Slag Binder and Its Interaction with Polycarboxylate Superplasticizer: Importance of Microstructural Design of the PCEs, (2022). https://doi.org/10.1021/acssuschemeng.2c05430.

[40] Y. Zhang, H.K. Chan, Z. Han, L. Lei, Why do conventional MAA-MPEG PCEs not work in alkali-activated slag systems?, Cem. Concr. Res. 184 (2024) 107599. https://doi.org/10.1016/J.CEMCONRES.2024.107599.

[41] J. Chen, J. Plank, Alkali-activated calcined clay blended cement: Effect of NaOH activator on performance of HPEG PCEs and on early strength, Cem. Concr. Res. 183 (2024) 107588. https://doi.org/10.1016/J.CEMCONRES.2024.107588.

[42] B. Rakhimbayev, B. Mukashev, P. Kusherova, A. Serikkanov, A. Kemelbekova, K. Agybayev, A. Aldongarov, N. Almas, Atomistic Insight on Effect of Silica Fume on Intermolecular Interactions between Poly(carboxylate) Superplasticizer and Calcium Ions in Concrete, Nanomaterials 14 (2024). https://doi.org/10.3390/nano14131084.

[43] A. Habbaba, J. Plank, Interaction Between Polycarboxylate Superplasticizers and

Amorphous Ground Granulated Blast Furnace Slag, J. Am. Ceram. Soc. 93 (2010) 2857–2863. https://doi.org/10.1111/j.1551-2916.2010.03755.x.